T.C.
NECMETTİN ERBAKAN UNIVERSITY
INSTITUTE OF SCIENCE

ANALYSIS OF THE ROLE OF BODIPY-BASED G-QUADRUPLEX STABILIZER ON TRANSLATIONAL AND TRANSCRIPTIONAL REGULATION

Cihad ÖZDEMİR

MASTER'S THESIS

Department of Molecular Biology and Genetics

December-2024
KONYA

THESIS APPROVAL AND ACCEPTANCE

The thesis entitled “Analysis of the Role of Bodipy-Based G-Quadruplex Stabilizer On Translational and Transcriptional Regulation” prepared by Cihad ÖZDEMİR, has been accepted as a MASTER'S THESIS in the Department of Molecular Biology and Genetics at Necmettin Erbakan University, Institute of Science, with consensus by the following jury on 18/12/2024.

Jury Member	**Signature**
Chair Assist. Prof. Tuğba Nur Aslan	……..
Advisor Assoc. Prof. Dr. Sündüs Erbaş ÇAKMAK	……..
Member Assist. Prof. Fatma Seçer Çelik	……..

Approved by the Institute of Science Administrative Board on …./…/20.. with the decision number ……..

Prof. Dr. Havvanur UÇBEYİAY
Institute Director

This thesis study was supported by the Necmettin Erbakan University Scientific Research Coordination Unit, project number 23GÜAMER03001.

TEZ BİLDİRİMİ

Bu tezdeki bütün bilgilerin etik davranış ve akademik kurallar çerçevesinde elde edildiğini ve tez yazım kurallarına uygun olarak hazırlanan bu çalışmada bana ait olmayan her türlü ifade ve bilginin kaynağına eksiksiz atıf yapıldığını bildiririm.

DECLARATION PAGE

I hereby declare that all information in this document has been obtained and presented in accordance with academic rules and ethical conduct. I also declare that, as required by these rules and conduct, I have fully cited and referenced all material and results that are not original to this work.

Cihad ÖZDEMİR

Tarih: 02.12.2024

ÖZET

YÜKSEK LİSANS TEZİ

BODIPY-TEMELLİ G-KUADRUPLEKS STABİLİZATÖRÜNÜN TRANSKRİPSİYONEL VE TRANSLASYONEL DÜZENLEMEDEKİ ROLÜNÜN İNCELENMESİ

Cihad ÖZDEMİR

Necmettin Erbakan Üniversitesi Fen Bilimleri Enstitüsü

Moleküler Biyoloji ve Genetik Anabilim Dalı

Danışman: Doç. Dr. Sündüs Erbaş Çakmak

2024, 67 Sayfa

Jüri

Doç. Dr. Sündüs Erbaş Çakmak

Dr. Öğr. Üyesi Tuğba Nur Aslan

Dr. Öğr. Üyesi Fatma Seçer Çelik

Gen ekspresyonu çeşitli seviyelerde ve şekillerde düzenlenebilir. Gen ekspresyonunu düzenleme yollarından biri de, G-dörtlü yapılarının stabilizasyonudur. G-dörtlüleri, hidrojen bağlı guanin tetrad düzlemlerinin istiflenmesi ile guanince zengin bölgelerde oluşan DNA ve RNA yapılarıdır. Bu yapılar, transkripsiyon ve translasyon gibi süreçleri etkileyerek gen ifadesinin düzenlenmesinde kritik bir rol oynar. Özellikle bazı kanser türlerinde EGFR'nin ekspresyonunun önemli ölçüde arttığı bilinmektedir. Bu tezde, G-dörtlü yapılarına bağlanabilen stabilizatör ile gen ekspresyonunun düzenlenmesi ve kanser hücrelerinin EGFR ekspresyonunun bundaki etkisi çalışılmıştır. Bunun için, G-dörtlü yapılara bağlanabilen BODIPY temelli bir ajan kullanışmıştır. Bu ajanın farklı EGFR ifadelerine sahip kanser hücrelerinde bulunan bazı onkogenlere etkisi transkripsiyonel ve translasyonel açıdan değerlendirilmiştir. Ayrıca, hücre hatlarındaki EGFR ekspresyonunu aynı zamanda floresan mikroskobu ile de tespiti için EGFR'ın tirozin kinaz alanını bağlanabilen erlotinib molekülü ile türevlendirilmiş BODIPY temelli bir görüntüleme ajanı sentezlenmiş ve hücrelerin rölatif EGFR seviyeleri belirlenmiştir. Bu çalışma kapsamında ilk kez BODIPY yapısındaki G4 stabilizatörün translasyon ve transkripsiyonel etkisi EGFR seviyesi işe karşılaştırılmıştır. Stabilizatörün EGFR RNA seviyesinde önemli bir azalışa neden olduğu ilk kez tespit edilmiştir. Diğer taraftan c-MYC protein seviyesinin 1 μM G4 stabilizatörü varlığında azaldığı gösterilmiştir. Elde edilen bulgular, BODIPY-temelli G4 stabilizatörlerinin kanserle ilişkili yolaklara olan etkisini ve anti-kanser terapötik potansiyelinin olduğunu göstermektedir.

Anahtar Kelimeler: BODIPY, EGFR, Gen ekspresyonunun düzenlenmesi, G-quadruplex, Kanser

ABSTRACT

MS THESIS

ANALYSIS OF THE ROLE OF BODIPY-BASED G-QUADRUPLEX STABILIZER ON TRANSLATIONAL AND TRANSCRIPTIONAL REGULATION

Cihad ÖZDEMİR

THE GRADUATE SCHOOL OF NATURAL AND APPLIED SCIENCE OF NECMETTİN ERBAKAN UNIVERSITY
THE DEGREE OF MASTER OF SCIENCE
IN MOLECULAR BIOLOGY AND GENETİCS

Advisor: Assoc.Prof. Dr. Sündüs Erbaş ÇAKMAK

2024, 68 Pages

Jury

Assoc. Prof. Dr. Sündüs Erbaş ÇAKMAK

Assist. Prof. Tuğba Nur Aslan

Assist. Prof. Fatma Seçer Çelik

Gene expression can be regulated at various levels and in various ways. One of the ways to modulate gene expression is by using G-quadruplex folds. G-quadruplexes are observed in G-rich sequences of nucleic acids and formed by stacking of hydrogen-bonded guanine tetrad planes. These structures play a critical role in regulating gene expression by influencing transcription and/or translation. It is known that the expression of EGFR is significantly increased in some cancer types. In this thesis, the regulation of gene expression by agents that can bind to G-quadruplex motifs and the effect of EGFR expression in cancer cells on this were studied. For this purpose, a BODIPY-based G-quadruplex stabilizer that can bind to G-quadruplex structures is used. The effects of this agent on some oncogenes in cancer cells with different EGFR expressions were evaluated in terms of transcriptional and translational aspects. In addition, a BODIPY-based imaging agent was synthesized using the erlotinib molecule, which is known to bind to the EGFR kinase domain, to detect EGFR expression in cell lines with fluorescence microscopy. Translational and transcriptional effects of G4 stabilizer in cell lines with different EGFR expression levels were compared. For the first time, BODIPY G4 stabilizer was shown to reduce mRNA level of EGFR. 1 μM stabilizer significantly reduced the c-MYC protein level. The findings point out the effect of BODIPY-based G4 stabilizer on cancer associated pathways and its therapeutic potential.

Keywords: BODIPY, Cancer, G-quadruplex, EGFR, Regulation of gene expression

ACKNOWLEDGMENT

I would like to extend my sincere gratitude to Necmettin Erbakan University Scientific Research Projects Unit for their support in this thesis study, and to TÜBİTAK for their support throughout my Master's education.

I am deeply grateful to Assoc. Prof. Dr. Sundus Erbaş ÇAKMAK for her guidance, mentorship, and the invaluable experience I gained from her throughout my Master's education.

I also thank Dr. Safaa Altves for her experimental support. I would like to express my appreciation to my labmates Betül Altunkaynak, Beyza Başar, Beyza Özçelik, Elif Çetli, Emin Şahin, Gökçe Özsamur, İlayda Öz, and all the SEC lab team.

Cihad ÖZDEMİR
December, 2024

CONTENTS

SYMBOLS AND ABBREVIATIONS

Symbols:

mL: mililiter

μL: microliter

nm: nanometer

μM: Micromolar

mM: Milimolar

MHz: Mega Hertz

Abbreviations:

ANOVA: One-Way Analysis of Variance

ATP: Adenosine Triphosphate

BCL-2: B-Cell Lymphoma 2

BODIPY: Boron-Dipyrromethene

c-Myc: Cellular Myelocytomatosis Oncogene

DAPI: 4',6-Diamidino-2-Phenylindole

DMEM: Dulbecco's Modified Eagle Medium

DMSO: Dimethyl Sulfoxide

DNA: Deoxyribonucleic Acid

dsDNA: Double-Stranded DNA

ECL: Enhanced Chemiluminescence

EGFR: Epidermal Growth Factor Receptor

FBS: Fetal Bovine Serum

FGF2: Fibroblast Growth Factor 2

FITC: Fluorescein Isothiocyanate

G4: G-Quadruplex

G4s: G-Quadruplexes

GAPDH: Glyceraldehyde-3-Phosphate Dehydrogenase

Hep3B: Hepatocellular 3B (Human Liver Carcinoma Cell Line)

HG-DMEM: High Glucose Dulbecco's Modified Eagle Medium

HRP: Horseradish Peroxidase

IRE: Iron-Responsive Elements

MCF-7: Michigan Cancer Foundation-7 Cell Line

MTT: 3-(4,5-Dimethylthiazol-2-yl)-2,5-Diphenyltetrazolium Bromide

NF: Nuclease-Free

NSCLC: Non-Small Cell Lung Cancer

ORF: Open Reading Frame

PDS: Pyridostatin

PeT: Photoinduced Electron Transfer

PFA: Paraformaldehyde

PQS: Putative Quadruplex Sequences

PVDF: Polyvinylidene Fluoride

qPCR: Quantitative Polymerase Chain Reaction

rG4s: RNA G-Quadruplexes

RNA: Ribonucleic Acid

RIPA: Radio-Immunoprecipitation Assay Buffer

SD: Standard Deviation

SDS-PAGE: Sodium Dodecyl Sulfate-Polyacrylamide Gel Electrophoresis

SSC: Side Scatter (in Flow Cytometry)

SSC-A: Side Scatter Area

SW480: Southwest 480 (Human Colon Adenocarcinoma Cell Line)

TBST: Tris-Buffered Saline with Tween 20

TFA: Trifluoroacetic Acid

T_m: Melting Temperature

TSS: Transcription Start Site

UTR: Untranslated Region

WB: Western Blot

ΔΔCt: Delta Delta Threshold Cycle

1. INTRODUCTION

Expression, regulation and function of genes differ among tissues and cell types and during various stages of development. For this reason, most of the diseases are known to be associated with abnormal gene expression. In fact, starting from the early developmental stages, expression of genes is dynamically regulated through epigenetic modifications. Gene expression can be controlled at many stages of transcription and translation. Therefore, regulation of these steps is of great importance for scientific and therapeutic reasons. One of the many factors that provide regulation of gene expression is G-quadruplex structures. G-quadruplexes (G4s) are non-canonical nucleic acid structures made up of four guanine bases stacked in a square planar pattern known as G-quartets, which are linked together by Hoogsteen hydrogen bonds (Burge et al., 2006). Metal cations, mainly monovalent ions such as Na^+ or K^+, influence the formation of G4 structures (Bhattacharyya et al., 2016). Due to the strong bonds among them, they are much more difficult to unfold compared to Watson-Crick base pairs (Watson & Crick, 1953). These structures are distributed in different regions of DNA, such as in the promoters of genes, open reading frames (ORFs) and telomeres. Keeping G4s stable can help treat some defective cell functions associated with overexpression of certain genes, by inhibiting the expression of these genes. Using these structures for gene control is a promising approach, especially in diseases associated with overactivated oncogenes. Although the entire function of structures is yet to be known and there are some studies and challenges regarding their therapeutic use, G-quadruplex stabilizers are promising agents that may play a role in the regulation of gene expression and translation (Baser et al., 2023).

Several molecules have been discovered that can stabilize G-quadruplexes. In recent years, boron-dipyrromethene (BODIPY) is also used for that purpose, which is also a potent fluorescent dye (Uyar et al., 2023; Baser et. Al. 2023). In this thesis, the translational role of a BODIPY-based G-quadruplex stabilizer, previously developed by Erbas-Cakmak research group, is examined and dependence of gene expression on Epidermal Growth Factor Receptor (EGFR) level is deduced (Baser v.d., 2023). EGFR receptor expression level is deduced by a novel probe, an erlotinib modified BODIPY dye. The BODIPY molecule is linked to the erlotinib molecule, a FDA approved quinazoline derivative used as a tyrosine kinase inhibitor, via click reaction (Kolb et al.,

2001). In this manner, EGFR expression in cell lines is detected by fluorescence microscopy and flow cytometry.

EGFR is a membrane receptor belonging to the receptor tyrosine kinase family. The receptor regulates cell growth, survival, and proliferation. Its dysregulation is commonly linked to a variety of cancers. The BODIPY G-quadruplex stabilizer, with a planar structure, has extended conjugated structure with pyridinium moieties enabling interaction with G4 plane of nucleic acids (Zhao et al., Baser et. Al. 2024). The transcriptional and translational effect of this compound is investigated in different cells having different EGFR expression profiles.

2. LITERATURE REVIEW

2.1. Translational Regulation and Biological Importance

Differential expression and regulation of genes are essential for cellular functions that are fundamental to life, such as cell growth and differentiation. Regulation of gene expression allows cells to perform their functions spatiotemporally. Gene expression can be regulated in many ways, including transcription, RNA processing, mRNA transport, translation, and post-translational chemical modifications. Translational control is the last and most important step in gene expression because it transfers information from mRNA to protein. Translational control is important because cells may swiftly and dynamically change protein synthesis. This is especially important when cells must respond fast to stress, nutritional deficits, growth cues, or other environmental changes.

Gene expressions can be modulated in various ways at the translational level. In translational level regulations, mRNA level is not directly affected. It is used by the cell for maintaining cellular homeostasis, responding to environmental effects, responding to stress conditions, and some developmental differentiations. There are several ways that translational control works. Ribosome interaction with the mRNA and the start of translation are influenced by particular sequences and structural components in the 5' and untranslated 3' UTR region of mRNA. For instance, ferritin mRNA's 5' UTR consist of iron-responsive elements (IREs) that modulate translation based on intracellular iron levels. Proteins that bind to IREs dissociate at high iron concentrations, increasing ferritin translation and accumulating intracellular iron (Hentze et al., 1987).

Translational control is also significantly influenced by RNA-binding proteins and microRNAs (miRNAs). miRNAs can attach to target mRNAs, decrease their stability, or stop them from translating. The lin-4 miRNA, for instance, regulates developmental time in Caenorhabditis worms by preventing the lin-14 mRNA translation (Lee et al., n.d.). RNA-binding proteins also affect the translation efficiency and stability of mRNA. For instance, the HuR protein increases the stability and promotes translation of some mRNAs by binding to their 3' UTR (Brennan & Steitz, 2001a).

Modification of translation initiation factors is another way of ensuring translational control. For translation to begin in eukaryotic cells, various initiation factors

must work in harmony. Translation can be controlled in a way that affects the expression of many proteins, both gene-specifically and generally.

One of the mechanisms of gene control at the translational level is the modulation of initiator factors that enable mRNA to combine with the ribosome. The phosphorylation of eIF2α, can be given as an example of such a control mechanism. When stress conditions cause eIF2α to be phosphorylated, the formation of the GTP-tRNA^Met complex required for translation stops or slows down (medicine & 2007, n.d.). Phosphorilation of eIF2α causes a decrease in protein synthesis under cellular stress. Phosphorylation of eIF2α is increased in some amino acid deficiencies. In this case, it can also cause an increase in the translation of some specific genes required to cope with stress (Wek et al., n.d.). Another element that helps translational control is some structural elements on mRNA. Untranslated UTR regions can serve as binding sites for regulatory proteins and affect translation efficiency (Hentze et.al., 1996). RNA binding proteins (RBPs) further contribute to translational control by interacting with specific mRNA sequences or structures. For example, the ELAV proteins can bind to the 3' UTRs of mRNAs rich in AU and stabilize them. This has been shown to enhance translation(Brennan & Steitz, 2001b; Fan et. al. 1998). Furthermore, ELAV proteins have been shown to be essential for neuronal development in Drosophila melanogaster and the importance of RBPs for development has been shown (Robinow et al., 1988).

Considering that the ongoing translation process will end in failure in the absence of various amino acids, controlling this process before it starts is a logical control method that provides efficient use of energy and many other benefits. Translational control has several biological applications. Translational control offers a quick and energy-efficient adaptation in cells' stress response. For instance, when cells face heat shock, they increase the translation of heat shock proteins (HSPs) while decreasing total protein synthesis. By aiding in the refolding of denatured proteins, HSPs promote cell survival (Lindquist, 1986; medicine & 2007, n.d.). Translational control is important for embryonic cell differentiation and tissue creation in developmental processes. In the Drosophila melanogaster embryo, translational regulation of nanos mRNA is required for posterior axis development. Nanos mRNA becoming translationally active solely in the embryo's posterior region, to make sure embryonic development occurs properly (Gavis et al., 1994).

Translational control is an important process in nerve cells that regulates synaptic plasticity and memory. Translation of mRNAs occurred at synapses ensures the local synthesis of proteins based on synaptic activity. This is critical for enhancing or reducing synapses in the memory and learning processes (Kang & Schuman, 1996).

The pathogenesis of some diseases is due to problems in translational control. In cancer, defects in translational control mechanisms cause cell proliferation and accelerate tumor formation. High expression of translation initiation factors (i.e. eIF4E) causes excessive translation of oncogenic mRNAs and tumor progression (Benedetti et al., 2004). For these reasons, translational control mechanisms are considered as potential drug targets in the treatment of cancer. Translational control is also closely related to neurodegenerative diseases. In Alzheimer's as well as Parkinson's diseases, errors in protein folding and processing lead to the accumulation of dysfunctional proteins and cellular damage.

Cells respond to stress by using translational control mechanisms, including eIF2α phosphorylation. Nevertheless, continued stimulation of these systems under chronic stress might impair synapse function and memory formation (Moreno et al., 2012). In general, the regulation of developmental processes, homeostasis maintenance, and cell adaptability to environmental changes all depend on the translational control of gene expression. Regulation mechanisms allow cells to respond rapidly to changes without the need for transcriptional regulation. By fine-tuning translation, cells maintain homeostasis, adapt to stress, ensure proper development, and perform specialized functions such as synaptic plasticity. Disruptions and problems in these regulatory pathways lead to many diseases, such as cancer and neurodegeneration. Understanding these mechanisms provides valuable insights into cellular function and a thorough comprehension of translational control mechanisms might aid in the creation of novel therapeutic approaches for a range of pathological problems, including cancer and neurodegenerative or many other disorders.

Level of mRNA, its stability, localization, epigenetic modifications and access of it by the translational machinery all affect the translation. In the thesis work level of mRNA is aimed to be regulated by G4 stabilizers. Additionally, stabilization of RNA G4 structures is likely to affect protein production. The biological functions of G-quadruplexes including its effect on gene expression is described below.

2.2. G-quadruplex Structures

2.2.1. Definition and Structural Characteristics of G-quadruplexes

G-quadruplexes (G4s) are non-canonical nucleic acid folding structures made up of four bases of guanines stacked in a square planar pattern known as G-quartets. Guanines are linked together by Hoogsteen hydrogen bonds (Burge et al., 2006). Metal cations, mainly monovalent ions such as Na^+ or K^+, influence the formation of G4 structures in the G-quartet center (Bhattacharyya et al., 2016). G4s can adopt a variety of parallel, antiparallel and hybrid conformations. These structures can exist within a single nucleic acid strand (intramolecular) or between distinct strands (intermolecular), and their polymorphism adds to their numerous biological activities and possible therapeutic uses (Figure 2.1.) (Burge et al., 2006). G-quadruplex structures can occur in both DNA and RNA biomolecules. While DNA G4s have more topological variation, RNA G4s primarily adopt the parallel quadruplex conformation (Joachimi et al., 2009).

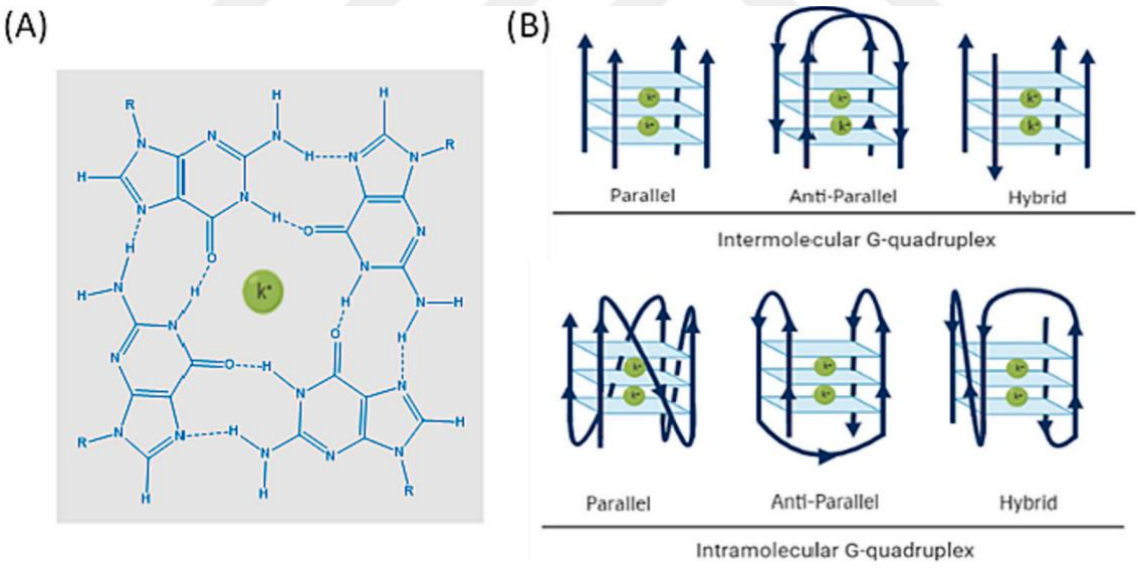

Figure 2.1. G4 structures. (A) Hydrogen-bonding guanines in the G-quartets and the potassium ion (K^+) at the center. (B) Different G4 topologies (Figueiredo et al., 2024).

Studies in many organisms have revealed that distribution of G4 motifs are not random but they are distributed in specific genomic regions (J. L. Huppert & Balasubramanian, 2005). In humans, yeast, and bacteria, G4 motifs are more concentrated in functional areas such as promoters (Capra et al., 2010; J. L. Huppert & Balasubramanian, 2005; Rawal et al., n.d.; Todd et al., n.d.). In addition, their genomic

location and nucleotide composition are conserved within human and yeast, suggesting an evolutionary advantage (Capra et al., 2010; Nakken et al., n.d.). The nonrandom localization of G4 motifs suggests that they have positive roles in cellular processes that are worth investigating. For example, telomeres have a high number of G4 motifs due to their GC-rich sequences and single-stranded overhangs. Moreover, these motifs are frequently found in G-rich micro- and minisatellites, around transcription start sites, within rDNA, near the binding sites of transcription factors, and at preferred sites of mitotic and meiotic double-strand breaks (Capra et al., 2010; Eddy et al., n.d.; Hershman et al., 2008; Nakken et al., n.d.). Their frequent presence in such regions points to G4s in genome stability, transcription regulation, and many other critical functions (Bochman et al., 2012).

Studies have shown that RNA G4 structures have many functions in the cell. For example, in neurons, RNA G4s can affect the localization of mRNA within the cell and regulate local translation (Subramanian et al., 2011). RNA G4s are also thought to play a role in the formation of stress granules (Chalupníková et al., n.d.; Subramanian et al., 2011; Valentin-Vega et al., 2016). RNA G4 structures can govern alternative splicing during the splicing process by interacting with splicing-directing proteins (Conlon et al., 2016; Huang et al., 2017). In addition, RNA G4 complexes might obstruct ribosomes during translation, reducing translation efficiency. G4-mediated translation inhibition has been demonstrated in several studies; in one study, a significant decrease in translation was noted when RNA G4s taken from the mRNA coding region of the FMRP gene were added to a luciferase reporter (Schaeffer et al., 2001; Varshney et al., 2020) .

2.2.2. G-Quadruplexes in the Genome and Their Biological Role

Several bioinformatic analyses and experimental methods are used to identify G-quadruplexes in the genome. By looking at the sequences, regions where four or more consecutive guanine nucleotides are aligned and short loop regions are located between them can be considered as potential G-quadruplex sequences (Todd et al., 2005). The mapping of G-quadruplex structures across the genome has been made possible by high-throughput sequencing techniques like G4-seq (Chambers et al., 2015). Researchers have found many G-quadruplex structures in the human genome with the G4-seq technique and have shown that they are denser in gene regulatory regions. In the analyses conducted

on the human genome, thousands of regions that can form potential G-quadruplexes have been identified (J. Huppert et al., 2005 and 2007). G-quadruplex structures can be seen in almost every region in the genome (Figure 2.2.).

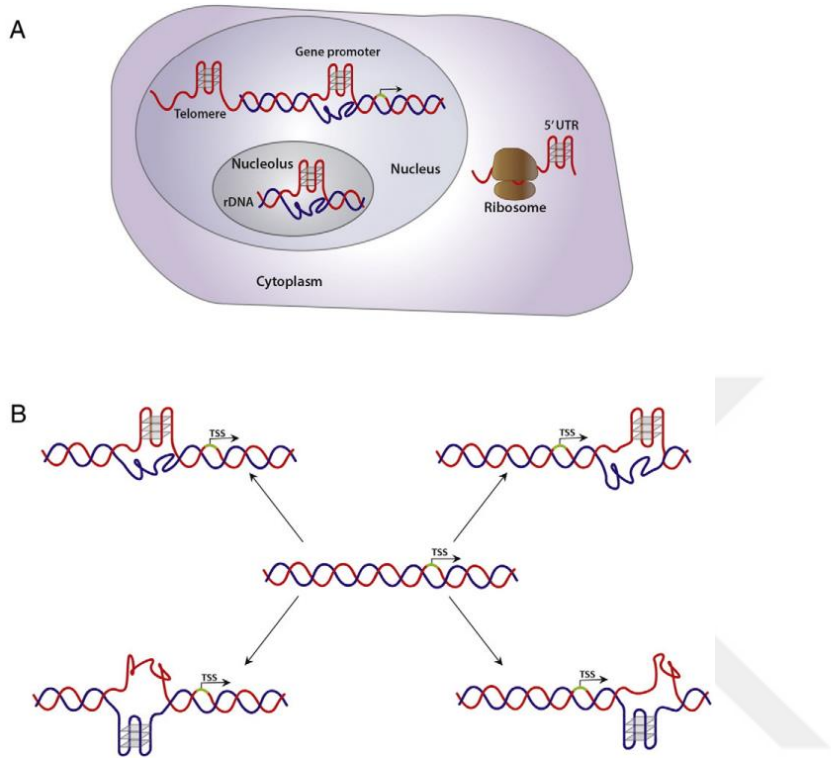

Figure 2.2. Distribution of probable G4 structures (A) and their possible position near the TSS (B) (Rigo et al., 2017; Smestad & Maher, 2015)

In general, the frequency of G-quadruplexes is higher in promoter regions. It has been observed that potential G-quadruplex sequences can be found in an estimated 40% of gene promoter regions in the genome (Figure 2.3.) (J. L. Huppert & Balasubramanian, 2007). This situation confirms the purpose of using G-quadruplex structures for transcriptional regulation. Since cancer is one of the diseases requiring urgent treatment, G-quadruplex structures, which are frequently found in the promoters of oncogenes and genes involved in cell signaling, are useful targets for therapeutic purposes. The transcriptional regulation effect of G-quadruplex structures is higher in the gene, especially in the promoter region. The presence of these structures in the promoter regions can seriously affect gene expression. In a study, G-quadruplexes located in the promoter region of the c-MYC oncogene showed a suppressive effect on gene transcription (Siddiqui-Jain et al., 2002). This structure occurs with the local opening of DNA and the subsequent formation of G-quadruplex. This situation limits the binding of transcription

factors and RNA polymerase II and the formation of complexes. Examples of genes that form G-quadruplexes include genes such as KRAS (Cogoi et al., 2006), VEGF (Sun et al., 2005), and BCL-2 (Dexheimer et al., 2006). The folding of G4 structures during replication may have an impact on how replication forks proceed. This is crucial for preserving the stability of the genome. However, the replication fork may break and double-stranded DNA may arise if helicases, which function as unwinders against G4 structures, are not present. It has been demonstrated that helicases like FANCJ and BLM, in particular, inhibit these harmful effects by unwinding G4 complexes (Wu and Brosh, 2010).

G-quadruplexes, which are also found in telomeric regions, help protect chromosome ends and are also involved in telomerase enzyme activity. By controlling telomerase activity, G4 structures at telomeres also contribute to cellular aging and cancer-related processes (Neidle et al., 2003). The presence of G-quadruplexes in these structures that provide stability to chromosomes may prevent telomerase from adding telomeres and thus affect some processes such as cell aging and lifespan (Neidle, 2017).

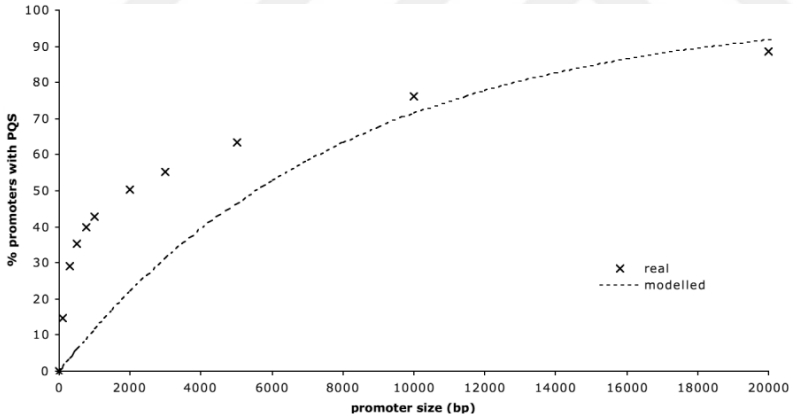

Figure 2.3. The distance of G quadruplex structures from the transcription start site."(J. L. Huppert & Balasubramanian, 2007)

G4 structures have also been shown to have various effects on signaling pathways. During stress, they can modulate the expression of protective genes. For instance, cellular defense systems can be enhanced by using ligands that maintain G4 structures under stress (Bugaut and Balasubramanian, 2012). Furthermore, G4 structures have been shown to influence chromatin structure and histone alterations as well as play a part in epigenetic control (Hänsel-Hertsch et al., 2017; Sarkies et al., 2010; Schiavone et al., 2014).

G-quadruplexes can also occur in RNA molecules and are called RNA G-quadruplexes (rG4). rG4s are found in various types of RNA, including mRNAs, long non-coding RNAs, and pre-mRNAs (Wieland et al., 2007). G-quadruplexes in RNA are generally more stable than in DNA because the 2'-hydroxyl group of RNA contributes to additional hydrogen bonds and stacking interactions (Sansalone et al., 2018). In RNA molecules, G-quadruplexes are frequently encountered in untranslated regions, especially in the 5' UTR and 3' UTR. G4 structures in the 5' UTR play a regulatory role in protein synthesis by preventing the ribosome from binding to the mRNA and the initiation of translation (Figure 2.4.) (Beaudoin et al., 2010). For example, a G-quadruplex located in the 5' UTR of the NRAS proto-oncogene has been demonstrated to inhibit translation of this gene (Kumari et al., 2007). rG4 structures in the 5' UTR can reduce protein synthesis by restricting the movement of the ribosome on the mRNA (Bugaut et al., 2012). An rG4 located in the 5' UTR of the fibroblast growth factor 2 (FGF2) mRNA is one of the important structures that regulate translation of this gene (Bonnal et al., 2003). When we look at the G-quadruplexes in the 3' UTR, translational efficiency, localization, and mRNA stability can all be impacted by some G-quadruplexes in the 3' UTR (Arora & Suess, 2011). These structures can interact with microRNAs, then RNA-binding proteins are affected.

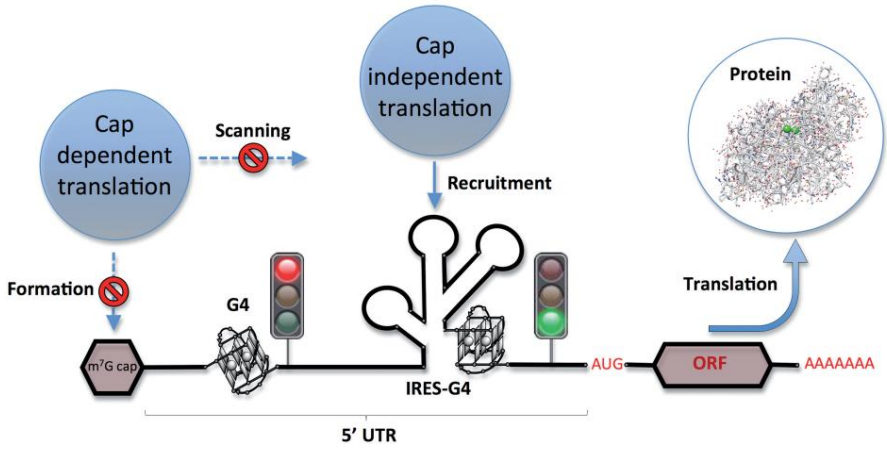

Fig. 2.4. Potential functions of 5'-UTR RNA G-quadruplex production in the regulation of translation initiation. The red refers to inhibition of translation. Green refers to improved translation. (Bugaut et al., 2012)

In addition, rG4s are also involved in alternative splicing processes. G-quadruplex structures in pre-mRNAs allow the recognition of splice sites and thus can modulate the formation of different protein isoforms (Marcel et al., 2011). The stability of G-quadruplexes generally depends on the number of G-tetrads, loop length and the presence

of monovalent cations (Hardin et al., 1993). As can be understood, G-quadruplexes can be found almost everywhere in the genome and can have regulatory effects at different levels of gene expression. They mostly play regulatory roles in gene expression by affecting transcription in promoter regions, translation in UTRs and RNA processing. The increasing amount of evidence supporting the G4s folds in the cells and their interference in regulatory role makes these structures appealing targets for drug development. In this regard, G4 may contribute to the development of new treatment and diagnostic approaches. Developing agents that can control the reading of mRNA is one strategy for influencing gene expression at the translational level (Figure 2.5). For instance, the G-quadruplex structure in the 5′-UTR of TRF2 mRNA inhibits translation in human cells (Gomez et al., 2010).

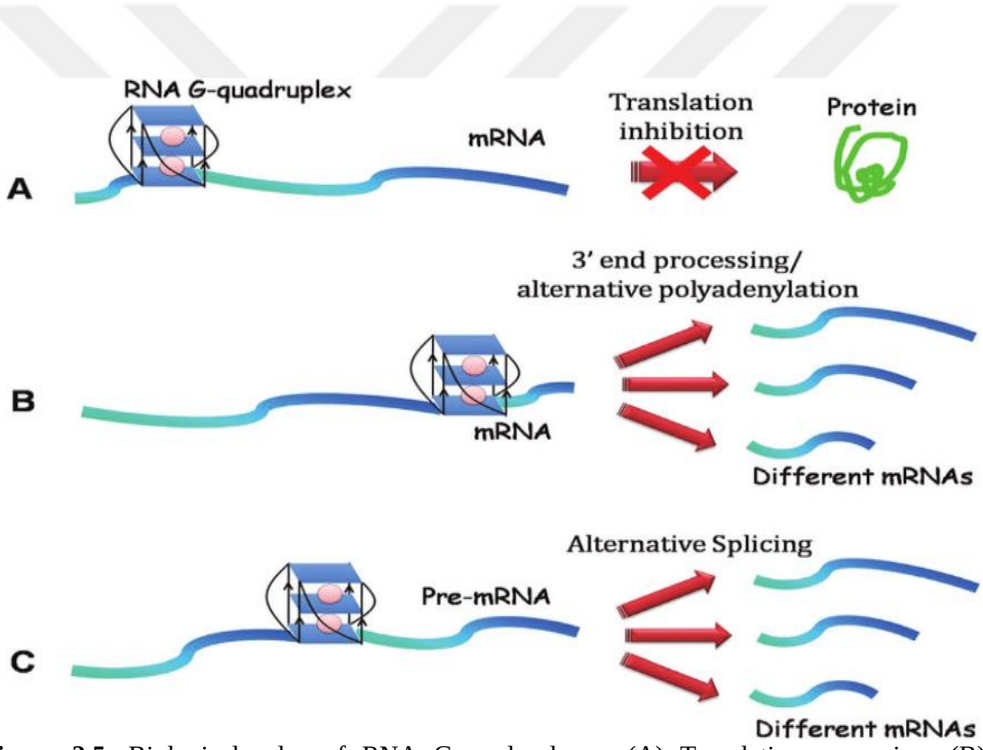

Figure 2.5. Biological roles of RNA G-quadruplexes. (A) Translation repression. (B) alternative polyadenylation, 3' end processing. (C) Alternative splicing. (Agarwala et al., 2015)

G4s can be found in many biological processes from gene regulation to genome stability. These structures improve our understanding of biological activities and bring up new avenues for molecular biology study. It is crucial to fully comprehend their biological significance to comprehend genetic mechanisms as well as develop effective treatment plans.

2.2.3. Therapeutic Potential of G-quadruplex Stabilizers

Keeping G4s stable can help treat some defective cell functions by inhibiting the expression of certain genes. Using these structures for gene control is a meaningful approach, especially in diseases associated with oncogenes.

By inhibiting the overexpression of oncogenes, G-quadruplex stabilizers are used in cancer treatment to limit cell growth (Neidle, 2017). The transcription and translation of important oncogenes, including c-MYC, KRAS, and BCL-2, are inhibited when G4 structures are stabilized in their promoter regions (Balasubramanian et al., 2011). In fact, there are some small molecules, drugs, and therapeutic approaches that target G4s. Agents that target G4s help increase their stability by binding to these structures with high affinity. For example, Pyridostatin (PDS) is a molecule that can bind to these structures and stabilize them. Thus, it affects gene expression at the transcriptional level. The promoter region targeted by PDS usually belongs to the c-MYC oncogene. This gene targets G4s in the promoter region and has gene suppressor properties (Müller et al., 2012). The TMPyP4 molecule can target G4 structures in DNA and RNA (Izbicka et al., 1999). Another molecule, CX-5461, may stabilizes G4s in DNA and causes apoptosis in BRCA1/2 mutated cancer cells (Xu et al., 2017). In diseases such as Alzheimer's and Parkinson's, where misfolded proteins form the basis, targeting RNA G-quadruplexes can change the course of the disease by altering the synthesis of these proteins (Simone et al., 2015). For example, the translation of tau proteins (tubulin associated unit proteins) can be prevented by targeting G4 structures found in their mRNAs (Su et al., 2014)

G-quadruplex stabilizers are being researched as possible treatments for further disorders. G4 structures are present in the genomes of RNA viruses, particularly the hepatitis C and HIV viruses, which cause viral infections (Perrone et al., 2017). By preventing viral multiplication and protein synthesis, stabilizing these structures may have antiviral effects. Important considerations in the improvement of G-quadruplex stabilizers include specificity and toxicity. Agents must have a strong affinity for the targeted G4 structures without interfering with regular cellular processes (Asamitsu et al., 2019). As a result, these characteristics are considered while developing new molecules.

G-quadruplex stabilizers are promising agents that may play a role in the regulation of gene expression and translation. They may help treat and control the

progression of certain diseases including cancer, neurodegenerative diseases and viral infections.

2.2.4. Current Limitations and Unmet Needs in Therapeutic Applications of G-quadruplex Stabilizers

For effective therapeutic use of G-quadruplex structures, the literature on these structures and especially their function in the cell needs to be expanded. Potentially capable of controlling gene expression in many different steps, more scientific studies are needed on the effects of these structures on translation. The potential benefits of G4s in translational control are interesting. However, there is a serious lack of information on translational regulation involving G4s. This lack of information covers some basic steps related to the formation, stability and translational control of G4 structures. In terms of literature, we see some limitations in addressing the lack of information on these structures. One of these is that G4 structures cannot be directly observed in vivo (Di Antonio et al., 2012). Studies on these structures are mostly conducted in vitro. The techniques we use to map G4 formation and distribution in vivo are not sufficient to reveal all of these structures. Fluorescent probes and antibodies are not fully adequate in terms of specificity and sensitivity (Biffi et al., 2013). And these techniques do not allow us to follow the dynamic changes of G4s in the cell. In addition, these types of techniques, which are widely used, cannot fully reveal how G4s affect ribosome progression or how they interact with the translational machinery (Varshney et al., 2020). And studies report different effects of these structures. For example, as mentioned before, it has been said that G4s prevent ribosome binding at the 5' UTR and can inhibit translation, but another study suggests that G4s can facilitate translation under certain conditions (Niu et al., 2022). Such situations suggest that G4s are complex structures in terms of function, which can play very different roles in translational control.

The conditions influencing the forming and stability of G4 structures in the cell are also poorly known. The cell's ionic environment has a substantial impact on G4 stability (Hazel et al., 2004). The creation and stability of G4 structures are determined mostly by the concentrations of potassium and sodium ions. However, there is little evidence about how ionic changes in the cell affect G4 development. Another significant drawback concerns the dynamic nature of G4 structures. G4 complexes develop and

dissolve quickly, depending on the cellular context and external factors. This makes it impossible to directly monitor their biological function. For example, the compounds employed to stabilize or destabilize G4 structures in vivo studies are frequently nonspecific, making it difficult to analyze G4 effects on translational control in isolation (Bugaut et al., 2012). Furthermore, the approaches utilized to detect whether G4 structures are physiologically stable or unstable have a limited sensitivity. NMR spectroscopy and single-molecule FRET can examine G4 structures in detail, but their use in a genetic and cellular setting is limited (Hänsel-Hertsch et al., 2017).

Another challenging situation is that the proteins associated with the presence and function of G4s in the cell have not been fully identified or their effects are unknown. Identifying these proteins is very important for better utilization of G4s. For example, G4 binding proteins can affect the stabilization and opening of G4 structures (Mendoza et al., 2016). For example, some helicases such as DHX36 have been shown to be involved in the unwinding of G4 structures (M. Chen et al., 2018). However, the way these proteins affect the control of translation is still not completely clear. There is limited information on how RNA G4 structures also affect translation. In addition, in order to increase the efficiency of the development of therapeutic molecules that affect RNA G4 structures, more studies need to be done on how these molecules are transported and distributed in the cell. According to current data, RNA G4 structures are found in regions such as the 5' untranslated region (UTR) and 3' UTR and it is known that these regions affect ribosome binding and translation. However, obtaining more data on the interaction of G4s with other regulatory mechanisms of translational control will help to develop more accurate therapeutic approaches because the interaction of G4s with microRNAs, RNA binding proteins and ribosomal subunits and its effect on translation efficiency is almost unknown (Rouleau et al., 2018). In addition, more advanced biomarkers and detection methods will help to better understand the therapeutic value of G4s. Advanced bioinformatics tools will be useful to predict the genomic locations of RNA G4s. Current tools are not sensitive enough. Efficient tools to measure RNA G4 stability in in vivo experiments will also facilitate the study of these structures. High-resolution imaging techniques and G4-specific antibodies can facilitate in vivo studies. Additionally, there are unmet requirements for the therapeutic use of G-quadruplex stabilizers. Ensuring the specificity and selectivity of G4 stabilizers is the main obstacle (Asamitsu et al., 2019). It is challenging to create a medication that targets a specific G4 structure since G4 structures

are found in many different parts of the genome and transcriptome. This may result in a higher risk of toxicity and off-target consequences. For instance, it may have unintended effects to target the G4 structures of oncogenes in cancer cells while simultaneously altering the G4 structures of essential genes in healthy cells (Neidle, 2017).

Another significant drawback for therapeutic uses is the pharmacokinetic and pharmacodynamic characteristics of G4 stabilizers. Due to their large molecular weight or polyanionic nature, many G4 binding ligands have trouble passing through cell membranes and getting to the target region (Collie et al., 2011). Furthermore, nothing is known about how these compounds are distributed, metabolized, and eliminated from the body. Determining suitable dosing schedules and treatment methods is challenging due to these shortcomings.

There is very little knowledge about the long-term effects of G4 stabilizers and possible resistance mechanisms. Cancer cells and other target cells may become resistant to G4 stabilizers or show adaptive responses (Richl et al., 2024; O'Hagan et al., 2019). This is a serious issue for the long-term effectiveness of therapies. Finally, the effects of G4 stabilizers on physiology and possible adverse effects are little known. Given that G4 structures have a role in various levels of gene expression, substantial manipulation of these structures has the potential to produce unwanted results (Müller & Rodriguez, 2014). As a result, more thorough toxicological and pharmacological research is necessary to ensure the safe and effective usage of G4 stabilizers.

Scope of the thesis involves the biological effects and hence therapeutic potential of BODIPY-based G-quadruplex stabilizer. Therefore, a brief literature regarding the BODIPY compounds are given below.

2.3. BODIPY Molecules

BODIPY (boron-dipyrromethene) is a type of fluorescent dye known for its good photophysical properties, photostability, and solubility in various solvents (Loudet & Burgess, 2007). These dyes have been widely used in fields such as molecular biology, nanomaterials, and imaging, sensing, and other purposes.

The boron-dipyrromethene (BODIPY) molecule is largely planar (Tram et al., 2009). Treibs and Kreuzer developed BODIPY in 1968, which comprises pyrrole, azafulvene, and diazaborine rings in a p-conjugated system (Treibs & Kreuzer, 1968).

BODIPY compounds can be functionalized with different groups to its cores and boron center, allowing for control over conjugation length and photophysical characteristics. BODIPY derivatives have high absorption, bright fluorescence, good stability, solubility (Y. Chen et al., 2012; Umasekhar et al., 2015). BODIPY is used in many applications such organic electronics, photodynamic treatment, and sensors (An et al., 2021; Bassan et al., 2021; Bulut et al., 2017; Chi et al., 2012; Liu et al., 2020; Merkes et al., 2021; Mikulchyk et al., 2022; Sansalone et al., 2018).

Strong fluorescence structure of BODIPY is found by accident in 1968. In this technique, brilliantly colored mono- and di-substituted BODIPY molecules were obtained (with less than 10% yield). The chelation of BF2 with dipyrrin produces a tetrahedral shape around the boron atom (Treibs & Kreuzer, 1968).

BODIPY dyes typically exhibit an absorption peak at 500 nm, but modification is necessary to obtain absorption in the near-infrared (NIR) area, which is the desired wavelength range for in vivo photodynamic therapy (PDT). Nowadays, BODIPY dyes are extensively researched in sensors, laser dyes, light cells, and biological applications (Yadav & Misra, 2023).

BODIPY dyes' spectroscopic characteristics may be expanded by adding the right groups to the core at suitable places. Boron dipyrrin dyes are readily functionalized at the pyrrole, the meso-position, and by changing the BF_2 bridge (Boens et al., 2015). The BODIPY structure may be derived using several functionalization approaches. Significant progress has been made with methods such as nucleophilic substitution, Knoevenagel condensation, substitution on boron, styrylation, nucleophilic substitution, cross-coupling reactions (Figure 2.6) (Zhu et al., 2013). All these strategies may be applied to the production of BODIPY derivatives to control their optoelectronic characteristics.

BODIPY conjugates can be designed to preferentially bind to G-quadruplex structures, acting as structural probes. They can aid in visualizing the formation and localization of G-quadruplexes in cells or in vitro. BODIPY conjugates can also be used to target drug delivery to G-quadruplex-containing regions (Uyar et al., 2023; Baser et al. 2023). By conjugating therapeutic agents with BODIPY dyes that bind specifically to G-quadruplexes, drugs can be delivered selectively to cancer cells or other disease-relevant targets where G-quadruplexes are abundant.

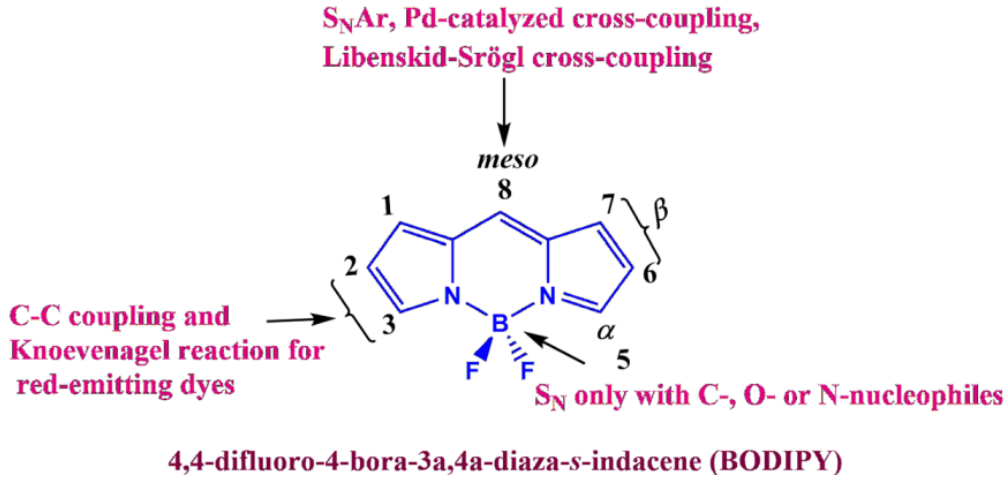

Fig. 2.6. BODIPY dye reactions and modifications (Yadav & Misra, 2023)

2.4. Epidermal Growth Factor Receptor

EGFRs are involved in various processes including cell growth, survival, and proliferation. Its dysregulation is commonly linked to a variety of cancers, with EGFR overexpression, mutations, or abnormal activation all contributing to tumor initiation, progression, and metastasis. EGFR signaling pathways influence key cellular processes such as proliferation, angiogenesis, and apoptosis resistance, making it an important target for cancer treatment. Inhibitors that target EGFR, such as tyrosine kinase inhibitors (TKIs) and monoclonal antibodies, have been developed and used to treat EGFR-driven cancers, resulting in better patient outcomes in some cases.

Since EGFR is a signal transduction pathway that plays a role in various biological processes such as cell growth, division and communication between cells, overexpression of this gene supports the rapid and uncontrolled division of the cell. Reducing or completely stopping the activity of this receptor can reduce uncontrolled cell division. Numerous drugs have been developed to suppress EGFR activity. For instance, erlotinib, a quinazoline derivative, is an approved tyrosine kinase inhibitor used in combination with gemcitabine to treat metastatic lung cancer (NSCLC) or metastatic pancreatic cancer. Erlotinib inhibits epidermal growth factor receptor (EGFR) activation by binding specifically to its adenosine triphosphate (ATP) binding sites, leading to repression of downstream signaling pathways (Moyer et al., 1997). Erlotinib inhibits cellular proliferation, angiogenesis, and metastasis. Beyond its approved indications, Erlotinib

has shown promise in ovarian cancer, head and neck cancer, and glioblastoma (Hirte et al., 2010; Anisuzzaman et al., 2017). In this thesis project, erlotinib modified BODIPY compound is used to visualize relative EGFR expression in different cells.

In addition, the most fundamental problems encountered with approaches targeting EGFR are that the designed molecules have low target specificity and that the receptor acquires resistance by decreasing its affinity for the drug after mutations. In this regard, several molecules are being designed that can bind even to common mutant forms of EGFR. Some of them bind irreversibly. But such drug candidates are highly toxic to healthy cells.

Relative effect of BODIPY G4 stabilizers on EGFR expressing cells are not studied yet. In the thesis, the role of EGFR in transcriptional and translational G4 mediated gene regulation is explored.

3. MATERIAL AND METHOD

As part of thesis project, a probe for EGF receptor is synthesized and characterized. Photophysical properties of the probe are determined. Cytotoxicity of this probe is determined. Relative EGFR expression levels of the cells are investigated using fluorescence microscopy and flow cytometry methods. Later, a BODIPY G4 ligand, known to stabilize G-quadruplex structures is synthesized according to literature procedures (Baser et. al. 2023). The cytotoxicity of the compound was investigated and the effect of this ligand on transcription and translation in different cells are investigated and the data is analyzed considering EGFR level. Experimental methods are given below.

3.1. Synthesis of the Compounds

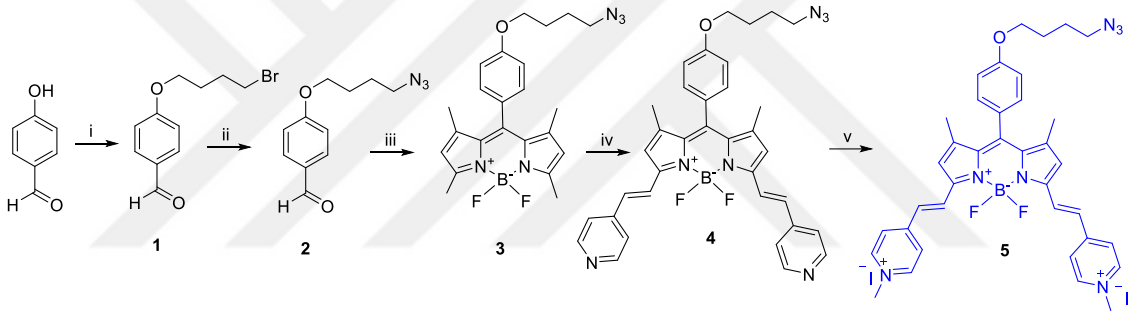

Scheme 3.1. Synthesis steps. i) DMF, K_2CO_3, dibromobutane; ii) DMSO, NaN_3; iii) DCM, 2.4-dimethyl pyrole, TFA, p-chloranil, Et_3N, BF_3OEt_2; iv) Benzene, 4-pyridinecarboxaldehyde, piperidine, AcOH; v) DMF, CH_3I.

The synthesis steps proceeded according to Scheme 3.1 using the procedures in literature (Baser et. al. 2023). Azide functionalized aldehyde is prepared in two steps followed by standard BODIPY synthesis using 2,4-dimethyl pyrrole. Knoavenagel condensation produced distyryl BODIPY compound, followed by pyridinium formation with methyl iodide. Nuclear Magnetic Resonance (NMR) spectra and QTOF-LC/MS spectra of the compounds are obtained for characterization, obtained from BİTAM at Necmettin Erbakan University. NMR spectra are given in the appendix part of the thesis. Purification of the compounds were done either through simple extraction, silica column chromatography or by precipitation. The synthesis of the probe, compound 6 was done using the compound 3 and erlotinib, through copper catalyzed click reaction with erlotinib EGFR binding module (Scheme 3.2).

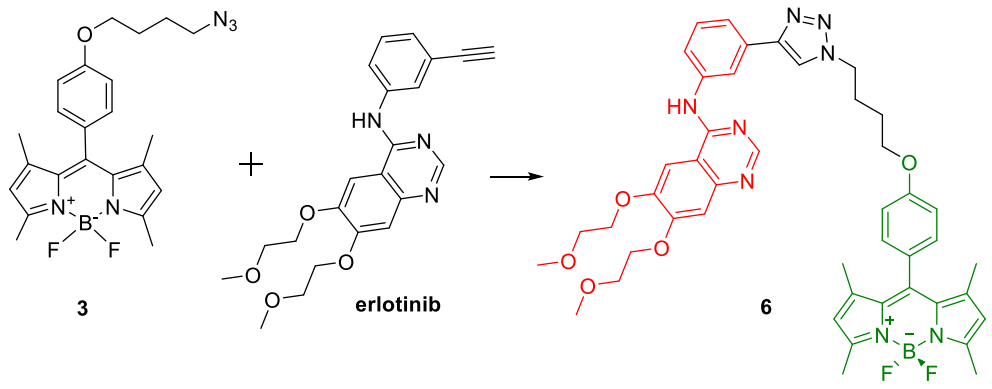

Scheme 3.2. Synthesis of compound 6. Reaction conditions: DMF, $MeCN_4Cu(I)PF_6$

3.1.1. Synthesis of the Compound 1

20 mmol 4-Hydroxybenzaldehyde (2.44 g) was dissolved in 20 mL dimethylformamide (DMF). 5.5 g of K_2CO_3 was added. 2 mol equivalents of dibromobutane (4.8 mL, 40 mmol) were added and the mixture was stirred at room temperature for 18 hours. After removing the solid part by filtration, the solvent was removed using a vacuum evaporator. The product mixture was extracted by using water and dichloromethane (DCM). The organic phase was collected, treated with sodium sulfate to dry it, and then the solvent was removed under vacuum. For purification, silica column chromatography with a hexane-ethyl acetate mixture (4:1 by volume) was used and a colorless oily product was obtained with a yield of 27%. NMR is consistent with the published data (Baser et. al. 2024).

3.1.2. Synthesis of the Compound 2

1.92 g of Compound 1 was dissolved in 12 mL of dimethyl sulfoxide (DMSO). 777 mg of sodium azide (1.5 equivalents) was added. The mixture was stirred at 60 °C for 3 h. After cooling the reaction to RT, dimethyl sulfoxide was removed by extraction with diethyl ether and water. The organic phase was collected and dried with Na_2SO_4, and then the solvent was removed under vacuum. The progress of the reaction was monitored using ^1H NMR spectroscopy, based on the shift of the proton adjacent to the bromine, and it was confirmed that compound 1 was completely consumed. A transparent gel-like substance was obtained with a yield of 98%. NMR is consistent with the published data (Baser et. al. 2024).

^{1}H NMR (400 MHz, Chloroform-*d*) δ 9.89 (s, 1H), 7.84 (d, *J* = 8.7 Hz, 2H), 6.99 (d, *J* = 8.7 Hz, 2H), 4.08 (t, *J* = 6.0 Hz, 2H), 3.39 (t, *J* = 6.7 Hz, 2H), 2.18 – 1.89 (m, 2H), 1.86 – 1.66 (m, 2H).

3.1.3. Synthesis of the Compound 3

1.6 grams of Compound 2 were dissolved in 100 mL of dichloromethane (DCM). Through the solution, N_2 was purged for 20 minutes. Then, 2,4-dimethylpyrrole (1.9 mL, 22.83 mmol) was added. 5 drops of trifluoroacetic acid (TFA) was added, and the solution was stirred under nitrogen gas at RT for 18 hours. 1.36 g of p-chloranil was added and stirred at room temperature for 2.5 hours. Triethylamine (7 mL, Et_3N) and borontrifluoride diethyl etherate (6 mL) were added successively and stirred at room temperature for another 2.5 hours. Extraction was performed with H_2O and DCM. The organic phase was collected and dried with sodium sulfate, and then the solvent was removed under vacuum. It was purified by silica column chromatography using a DCM-hexane mobile phase (4:3 by volume). A yield of 17% gave 550 mg of orange solid product. NMR is consistent with the published data (Baser et. al. 2024).

3.1.4. Synthesis of the Compound 4

Compound 3 (300 mg, 0.68 mol) was dissolved in 10 mL of benzene. Then, 2.06 mmol (194 µL) of 4-pyridine carboxaldehyde was added. 400 µL of piperidine and 400 µl of acetic acid were added. The reaction was stirred at 90 °C using the Dean Stark apparatus. During this time, the reaction was monitored by thin-layer silica chromatography, and the reaction continued until a green color was observed. When the color turned green and the product formed in thin-layer silica chromatography, the reaction was stopped, and the mixture was allowed to reach room temperature. Extraction was performed with H_2O and DCM. The lower DCM phase was collected and dried with sodium sulfate, and then the solvent was removed by rotary evaporator. It was purified by silica chromatography using an acetone-hexane mobile phase (3:1 by volume). The same procedure was repeated with the total amount obtained from silica chromatography. Using 420 mg of Compound 3 was recovered and 45 mg of Compound 4 was obtained with a yield of 7%. NMR is consistent with the published data (Baser et. al. 2024).

^{13}C NMR (101 MHz, $CDCl_3$) δ 159.73, 151.67, 150.34, 143.57, 143.27, 141.27, 133.20, 129.36, 126.60, 123.24, 121.34, 118.48, 115.20, 67.36, 51.20, 26.52, 25.77, 14.98.

3.1.5. Synthesis of the Compound 5

Compound 4 (45 mg, 0.072 mmol) was dissolved in 3 ml of dimethylformamide (DMF). Then, 0.5 mL iodomethane was added. It was left to stir at RT for the whole day. TLC was used for monitoring, and an additional 0.1 mL of iodomethane was added. After one more day of reaction, TLC checks were performed using a 10% methanol DCM system. DMF was evaporated, and purification was carried out by precipitation with ethyl acetate. Compound 5 was obtained with quantitative yields. NMR is consistent with the published data (Baser et. al. 2024).

^{1}H NMR (DMSO-d_6 , 400 MHz) δ 8.90 (d, *J* = 6.6 Hz, 1H), 8.20 (d, *J* = 7.1 Hz, 1H), 7.94 (d, *J* = 16.2 Hz, 1H), 7.83 (d, *J* = 16.3 Hz, 1H), 7.39 (d, *J* = 8.6 Hz, 0H), 7.23 – 7.11 (m, 1H), 4.32 (s, 2H), 4.11 (t, *J* = 6.3 Hz, 0H), 3.44 (t, *J* = 6.7 Hz, 0H), 1.83 (q, *J* = 6.6, 6.1 Hz, 0H), 1.78 – 1.66 (m, 1H), 1.55 (s, 1H).

3.1.6. Synthesis of the Compound 6

50 mg (0.115 mmol) of Compound 3 and 99 mg (0.23 mmol) of erlotinib were dissolved in 4 mL of dichloromethane (DCM). 43 mg (0.115 mmol) of $CuMeCN_4PF_6$ was added, and the reaction was left to stir at RT overnight. After one day, 50 mg of erlotinib, 50 mg of tetrakis-acetonitrile $CuMeCN_4PF_6$, and 1 mL of methanol were added, and the solution was stirred for 36 hours. After TLC analysis, extraction was performed with a 70 DCM: 30 propanol / saltwater mixture. The organic phase was not transparent, so another extraction was performed with pure water. A clear organic phase was obtained. The solvent was discarded through a rotary evaporator, and the material was purified in a column using a system of 3 acetone: 1 DCM: 1 hexane: 1 ethyl acetate. 97 mg of the first spot and 46 mg product was obtained with 46% yield.

^{1}H NMR (400 MHz, Chloroform-d) δ 8.53 (s, 1H), 8.12 (t, J = 1.9 Hz, 1H), 7.81 (dd, J = 2.3, 1.0 Hz, 1H), 7.79 (s, 1H), 7.51 – 7.42 (m, 1H), 7.36 (t, J = 7.9 Hz, 1H), 7.20

(s, 1H), 7.17 (s, 1H), 7.08 (d, J = 8.7 Hz, 2H), 6.91 (d, J = 8.7 Hz, 2H), 5.88 (s, 2H), 4.45 (t, J = 7.1 Hz, 2H), 4.28 – 4.15 (m, 4H), 3.98 (t, J = 6.0 Hz, 2H), 3.81 – 3.73 (m, 4H), 3.40 (s, 3H), 3.39 (s, 3H), 2.46 (s, 6H), 2.17 – 2.12 (m, 2H), 1.87 – 1.76 (m, 2H), 1.34 (s, 6H).

3.2. Spectroscopic Analysis of Compound 6

UV-Vis absorbance as well as fluorescence spectra of the compound 6 was recorded in DMSO. Using the reference compound Rhodamine 6G, quantum yield of compound 6 is calculated using the Formula 1 below:

$$Q = Q_R\ (I/I_R)*(A_R/A)*(n^2\ /n_R\ 2\ ) \qquad \text{Formula 1}$$

In the formula, Q_R refers to quantum yield of Rhodamine 6G reference, I and I_R refer to integrated emission of the sample and reference compound respectively when excited at 488 nm. A and A_R are absorbance values of compound 6 and reference compounds at 488 nm. Finally, n and n_R are solvent refractive indices. Compound 6 is dissolved in DMSO; therefore, n is taken as 1.4793. Rhodamin 6G is dissolved in water and the n for this solvent is 1.33. Quantum yield of Rhodamin 6G is taken as 0.95 (Magde et. al., 1999).

$$A= \varepsilon Cl \qquad \text{Formula 2}$$

The extinction coefficient was calculated using Beer-Lambert law, shown in Formula 2. A is the the absorbance, C refers to the concentration, whereas l is the light path (1 cm).

3.3. Cell Culture Experiments

All cells are human cells. MCF-7 (breast adenocarcinoma), HEP-3B (hepatocellular carcinoma), and SW480 (colorectal adenocarcinoma) cells were cultured in high glucose DMEM with 10% FBS and 0.5% gentamicin for 2 days to allow for cell

attachment. The culture media was changed every 2-3 days, and cells were monitored for confluency and general health under a microscope. When the cells reached 70-80% confluence, they were passaged by detaching them with trypsin-EDTA, centrifuging the suspension at 1200 rpm for 5 minutes, and reseeding them into fresh plates at appropriate densities. Cells were maintained in an incubator (humidified, at 37°C with 5% CO_2) throughout the experiments.

3.3.1. Cytotoxicity Analysis

We used MTT method for Cytotoxicity Analysis. MTT assay is used in cell biology and biochemistry. Metabolically active cells converted yellow tetrazole (MTT) into purple formazan crystals. This conversion occurred when mitochondrial enzymes, specifically succinate dehydrogenase, reduce MTT to its formazan molecules which are not soluble in water. The amount of formazan produced was correlated to the number of viable cells in a culture, making the MTT assay a popular method for determining cell viability, proliferation, and cytotoxicity in a variety of research and clinical settings.

First, the medium of the flask containing MCF-7, HEP3 and SW480 cells were removed. Then, cells were washed with PBS (1 mL), and PBS was discarded. Next, 1 mL of trypsin was added, and the cells were further incubated for 5 minutes at 37 °C. After that, 2 mL of HG-DMEM medium was added. All these cells were transferred to Falcon tube and centrifuged at 1200 rpm for 4 minutes. The supernatant was discarded, and medium was added (1 mL). Then, 20 μL of this medium was taken and added to an Eppendorf tube. 20 μL of trypan blue dye was added to this tube. The cells were counted using a Thoma cell counting chamber and about 5000 cells seeded equally into the wells of 96 well-plate. Incubation at 37 °C for 1 day follows.

For the cells incubated for 1 day, the desired amount of medium was prepared, and serial dilutions (0 μM-40 μM) were made. The Compound 5 and 6 agent solutions in culture medium were added to wells in different concentrations, with at least 3 replicates. The cells were then incubated at 37 °C for 1 day.

After 1 day of incubation, the medium was removed, then 90 mL new medium and 10 μL of MTT (The stock concentration is 5 mg/mL) was added to each well. The MTT procedure was carried out in the dark. The cells were then incubated at 37 °C for 4

hours. After 4 hours, the medium was removed, and 100 μL of DMSO was added to each wellto dissolve formazan crystals. The cells were put in the incubator for another 15 minutes. Finally, the absorbance at 570 nm was recorded using a microplate reader. Relative cell viability was calculated by normalizing the absorbance with respect to untreated cell control group.

3.3.2. Cell Imaging

Fluorescent cell imaging was performed by using erlotinib bearing compound 6 to examine EGFR expression in different cell lines. 5 μM Compound 6 was applied to HEP3B, MCF7, and SW480 cell lines to determine relative EGFR level of these cells.

The medium was removed from the cell flasks. Then, cells were washed with 1 mL of PBS and the PBS was discarded. The cells were counted using a Thoma cell counting chamber and seeded equally into each well. The cells were incubated for two days to allow full attachment. Cells were incubated with 5 μM of compound 6 for 1h at 37 °C. Then, the medium was removed from the wells. Each well was washed twice with 1 mL of PBS, and the PBS was discarded. 2 mL of 4% paraformaldehyde (PFA) was added to each well and covered with aluminum foil, then left at room temperature for 5 minutes. The solution was removed. Each well was washed twice with 1 mL of PBS, and the PBS was discarded. Cells were visualized using fluorescence microscopy (Zeiss). Images of the cells were analyzed using ImageJ software.

3.3.3. Flow Cytometry

To examine EGFR expression with erlotinib bearing compound 6, flow cytometry was performed for MCF7, and SW480 cell lines. For this purpose, 500,000 cells were seeded into the wells of a 6-well plate. The cells were incubated for one day. The cells were incubated with compound 6 for one hour. The medium was discarded, and the cells were washed with PBS. PBS was discarded. Then, 400 µL of trypsin was added and incubated for 5 minutes. 800 µL of medium was added. The groups were transferred to different Eppendorf tubes and centrifuged. After centrifugation, the cells were washed with PBS and centrifuged again. Finally, 500 µL of PBS and 1% FBS was added to each Eppendorf tube, and the samples were read on a flow cytometer. The fluorescence on FITC channel was recorded to track the fluorescence of compound 6. Data collected from 10,000 events per sample using a Beckman Coulter Cytoflex Cytometry. The fluorescence intensity was examined to determine relative EGFR expression and Compound 6 binding to EGFR receptors by comparing the control groups.

3.3.4. Quantitative Polymerase Chain Reaction (qPCR)

qPCR method was performed to measure the effect of compound 5 on the expression levels of target genes using qPCR. Cells (MCF-7, HEP3B, and SW480) were seeded at a density of $5x10^5$ cells/well in 6-well plates and incubated for 24 hours to allow for attachment and growth. Then, they were treated with compound 5 at given concentrations for 24 h. Non-treated cells used as control. Protocol recommended by the commercial RNA isolation kit was followed. The washed cell pellets were collected and homogenized in 500 mL of TRIzol reagent. The homogenate was incubated for 5 minutes at room temperature. Following incubation, 100 µL of chloroform was added to the homogenate, and the mixture was vigorously shaken for 15 seconds. The sample was then centrifuged at 10,000 rpm for 10 minutes at 4 °C. After centrifugation, the aqueous phase containing RNA was carefully separated and transferred to a fresh tube. RNA was precipitated by adding 500 µL of isopropanol, followed by incubation for 10 minutes at room temperature. The sample was then centrifuged at 10,000 rpm for 10 minutes at 4 °C, and the pellet was washed with 75% ethanol, air-dried and resuspended in RNase-free water. A Nanodrop device (Migrodigital, Nabi UV/Vis nano spectrophotometer) is

used to measure the concentration by measuring absorbance at 260 nm. The quality of RNA was determined by determining the A260/A280 ratio (ideally between 1.8 and 2.0). 1000 ng of RNA were taken by calculating according to the Nanodrop device concentration measurements. 1 µL DNase I and 1µL buffer were added to each. Volumes of samples with a total volume of less than 10 µL were completed to 10. They were kept at 37 °C for 30 minutes. 1 µL EDTA solution was added to all of them and kept at 65 °C for 10 minutes. RNA more than 1 µg was reverse transcribed into complementary DNA (cDNA) using Thermo Scientific, K1622 kit using to the protocol recommended by the kit; Firstly, the reagents (1 µg Template RNA, 1 µL Oligo $(dT)_{18}$ primer, 12 µg Water-nuclease-free) were added into a sterile, nuclease-free tube on ice. Then the mixture was mixed gently and centrifuged briefly. Then, 4 µL 5X Reaction Buffer, 1 µL RiboLock RNase Inhibitor, 2 µL 10 mM dNTP Mix and 1 µL RevertAid M-MuLV RT were added sequentially. Then, for cDNA synthesis using oligo$(dT)_{18,}$ the mixture was incubated at 42 °C for 60 min. After the reaction, the process was stopped by heating at 70 °C for 5 min. The reverse transcription was carried out with a combination of oligo(dT) primers.

Quantitative PCR was performed to assess gene expression levels. Specific primers for target genes (e.g., EGFR, c-myc, Bcl-2) and a housekeeping gene (GAPDH, β-actin) were used as shown in Table 3.1. A reaction mixture containing cDNA, primers, and SYBR Green master mix (Nucleogene, Turkey) was prepared according to the manufacturer's instructions. The qPCR was performed using Bio-Rad, CFX Connect device, and the following thermal cycling conditions were used: initial denaturation at 95°C for 10 minutes, followed by 40 cycles of denaturation at 95 °C for 15 seconds, annealed for 30 seconds, and extension at 72 °C for 30 seconds. Gene expression levels were quantified using the ΔΔCt method, where the threshold cycle (Ct) value of the target gene was normalized to the Ct value of the housekeeping gene. The relative expression was calculated as fold change compared to control samples.

Table 3.1. Real Time-qPCR primer sequences.

Gene	Forward Sequence (5'-3')	Reverse Sequence (5'-3')
β-ACT	CACCATTGGCAATGAGCGGTTC	AGGTCTTTGCGGATGTCCACGT
GAPDH	GAAGGTGAAGGTCGGAGTC	GAAGATGGTGATGGGATTTC
c-MYC	CCTGGTGCTCCATGAGGAGAC	CAGACTCTGACCTTTTGCCAGG
BCL-2	ATCGCCCTGTGGATGACTGAGT	GCCAGGAGAAATCAAACAGAGGC
EGFR	AACACCCTGGTCTGGAAGTACG	TCGTTGGACAGCCTTCAAGACC
VIM	AGGCAAAGCAGGAGTCCACTGA	ATCTGGCGTTCCAGGGACTCAT

3.3.5. Western-Blot Analysis

For Western Blot, MCF7 and SW480 cells were first cultured and treated with compound 5. After treatment, the cells were harvested and treated with ice-cold RIPA buffer containing Halt™ Protease Inhibitor Cocktail and inhibitors of phosphatase for 20 minutes at 4 °C. Then the sample was centrifuged at 10,000 rpm for 10 minutes at 4 °C, through which cell debris was removed. Bradford assay was used to determine protein concentration. 50- 100 µg of protein were mixed with a 6X Laemmli buffer with β-mercaptoethanol in it. Then for 5 min, sample was heated to 95 °C. SDS-PAGE, 10-15% polyacrylamide gel is used for separation. The proteins were transferred onto a PVDF membrane using a semi dry transfer system at 25V for 10 min. After transfer, the membrane was blocked with 3% non-fat milk in TBST for 1 hour at room temperature to avoid non-specific binding. The membrane was then incubated at 4 °C for about 16 h with the primary antibody (BCL2, c-MYC or β-Actin) diluted TBST as recommended by the kit. After washing with TBST, the membrane was incubated with a secondary antibody conjugated to HRP (horseradish peroxidase) for 2 hours at room temperature. Following washing, protein bands were detected using chemiluminescence (ECL) Thermo ECL Substrate and visualized with a chemiluminescent ChemiDoc Imaging System. The band intensity was quantified using Image Lab software, and the results were normalized to a housekeeping protein β-actin for comparison.

3.3.6. Statistical Analysis

Results of the replicates were plotted as mean data and standard deviations (SD) were included in the graph. To compare the groups statistically, unpaired t-test was used. If the p-value of the compared groups are less 0.05 ($p<0.05$), then the results are considered statistically significant.

4. RESULTS AND DISCUSSION

4.1. Synthesis and Characterization

Compounds were successfully synthesized with decent yields and characterized. NMR data of the compounds are given in the Appendix. Photophysical characterization of compound 6 was done to determine extinction coefficient (ε) and quantum yield of this compound. ε value was calculated to be 75000 $M^{-1}cm^{-1}$ at the peak absorbance value (501 nm) in DMSO. UV-Vis Absorbance and fluorescence spectra of the compound is given in Figures 4.1 and 4.2. The maximum emission wavelength of the compound was determined to be at 513 nm. Quantum yield is determined to be 0.81.

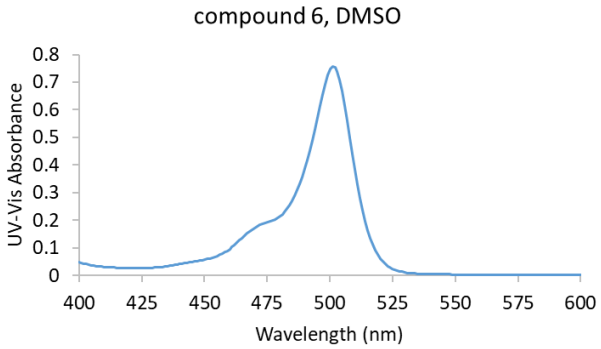

Figure 4.1. UV-Vis Absorbance spectrum of compound 6 in DMSO.

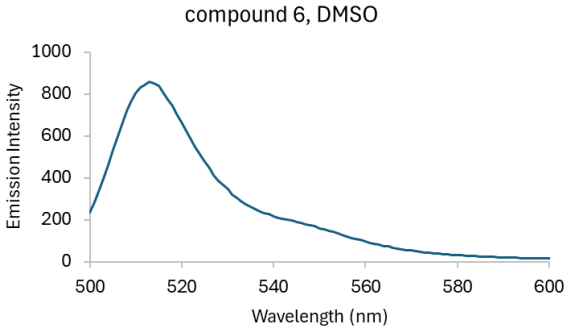

Figure 4.2. Emission spectrum of compound 6 in DMSO. The sample was excited at 500 nm.

4.2. Results of Cytotoxicity Analysis

The cytotoxicity of Compound 5 was investigated in colon and liver cancer cells which are SW480 and HEP3B respectively. MTT results indicate no serious cytotoxic effect in the cells treated with applied doses of Compound 5 and Compound 6 (applied dose is 5 μM or lower).

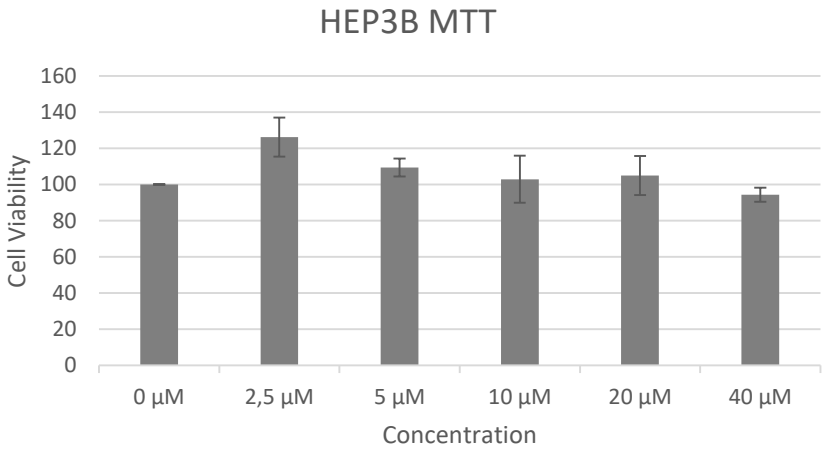

Fig. 4.3. Effect of compound 5 on the viability of HEP3B cells.

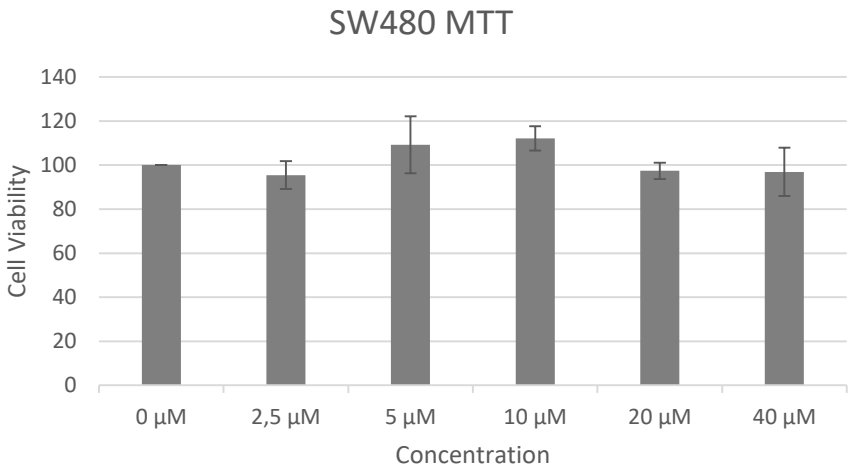

Fig. 4.4. Effect of compound 5 on the viability of SW480 cells.

IC50 value of compound 6 is higher than 160 μM for MCF7 cells (Figure 4.5). At 160 μM concentration cell viability is determined to be 65%. IC50 value of compound 6 is higher than 80 μM for SW480 cells (Figure 4.6). At 80 μM concentration cell viability

is determined to be 82%. For HEP3B cells viability in the presence of 160 μM compound 6 cell is 42% (Figure 4.7).

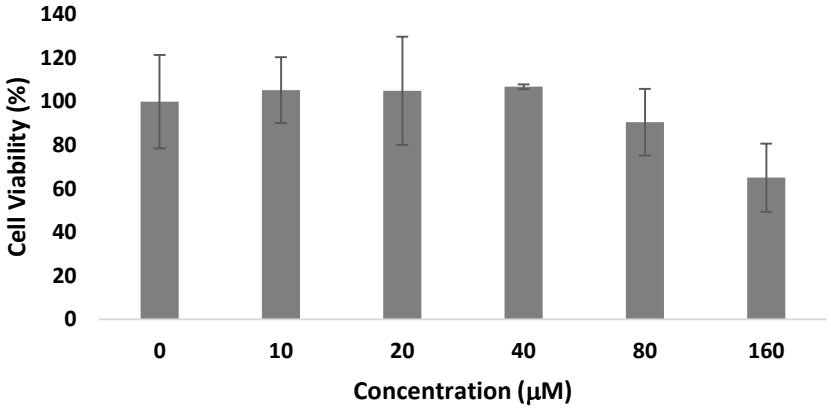

Fig. 4.5. Effect of compound 6 on the viability of MCF7 cells.

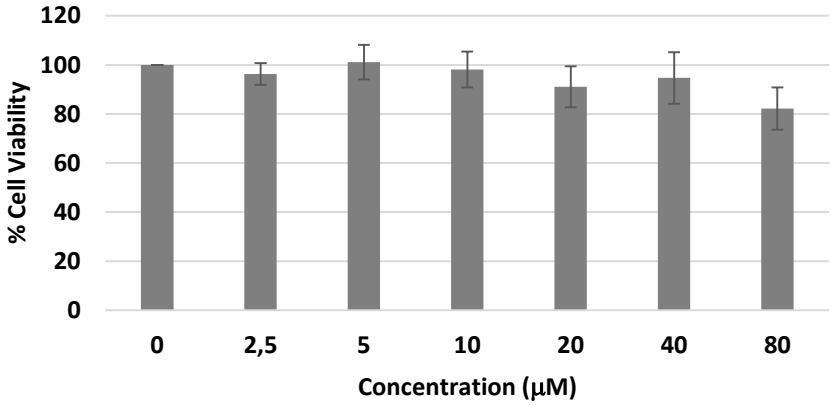

Fig. 4.6. Effect of compound 6 on the viability of SW480 cells.

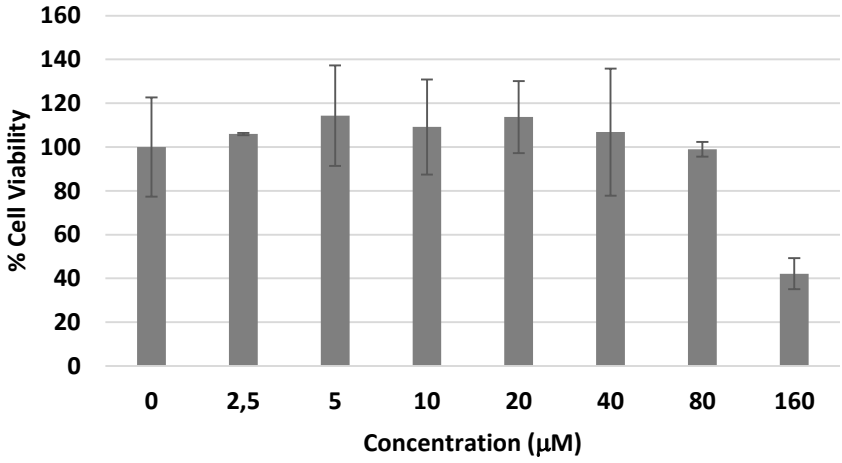

Fig. 4.7. Effect of compound 6 on the viability of HEP3B cells.

4.3. Results of Cell Imaging

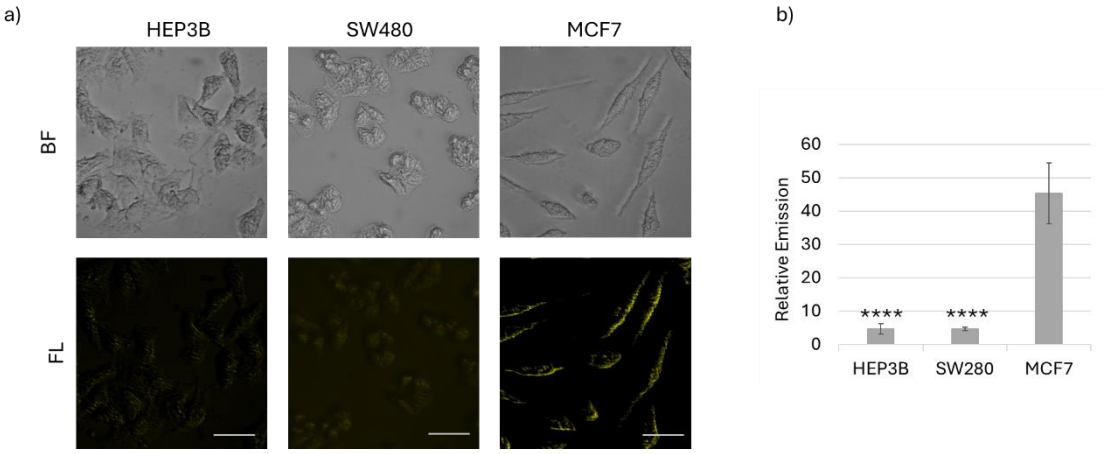

Fig. 4.8. Fluorescence images of HEP3B, SW480 and MCF7 cells incubated with compound 6 (5 μM) for 1h. **** $p \leq 0.0001$, n=4.

In all three cell lines treated with 5 μM Compound 6, fluorescence emission was recorded by fluorescence microscopy (Figure 4.8). EGFR expression levels were estimated from fluorescence intensities using ImageJ software. As shown in Figure 4.8-b, MCF7 EGFR level is significantly higher compared to other cells.

4.4. Results of the Flow Cytometry Analysis

According to the flow cytometry results, FITC signals, which corresponds to emission signal resulting from compound 6, were higher in the experimental group in MCF7 cells compared to SW480 as shown in Figures 4.9-4.11.

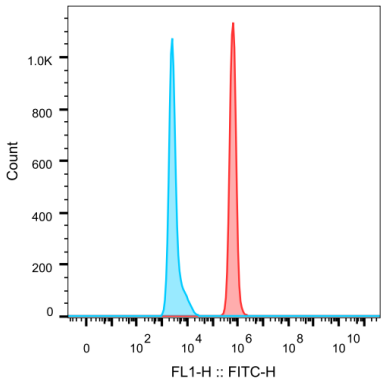

	Sample Name	Subset Name	Count
	MCF7 control	cells	8191
	MCF7 5 μM	cells	7534

Figure 4.9. Flow cytometry histogram showing the FITC-H fluorescence intensity of MCF7 cells.

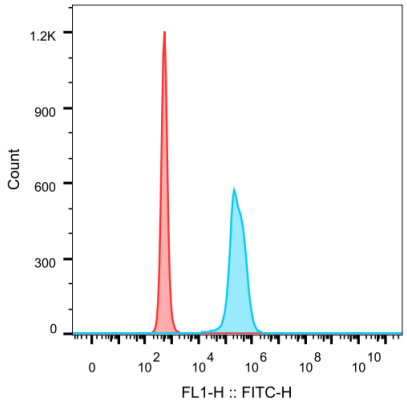

	Sample Name	Subset Name	Count
	Sw480 5 µM	cells	8423
	Sw480 Control	cells	7214

Figure 4.10. Flow cytometry histogram showing the FITC-H fluorescence intensity of SW480 cells.

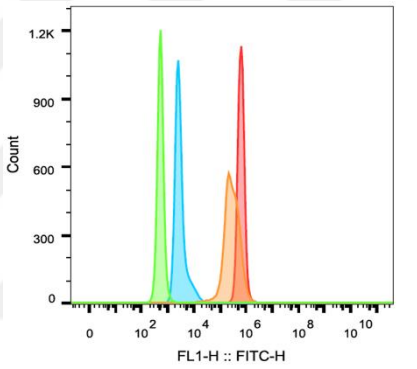

	Sample Name	Subset Name	Count
	Sw480 Control	cells	7214
	Sw480 5 µL	cells	8423
	MCF7 Control	cells	8191
	MCF7 5 µL	cells	7534

Figure 4.11. Flow cytometry histogram showing the FITC-H fluorescence intensity of both MCF7 and SW480 cells.

4.5. Results of Quantitative Polymerase Chain Reaction

The effect of compound 5 on the mRNA level of various genes in MCF7 cells were previously analyzed by Erbas-Cakmak research group (Baser et. al. 2023). Therefore, for this cell line, expressions of EGFR, BCL2 and c-MYC were analyzed. In certain cases, both β-Actin and GAPDH were used as housekeeping genes. In MCF7 cells treated with 5 µM compound 5, mRNA level of EGFR is shown to be significantly reduced by half (Figure 4.12). On the other hand, change in the expression of BCL2 is not significant (Figure 4.13.)

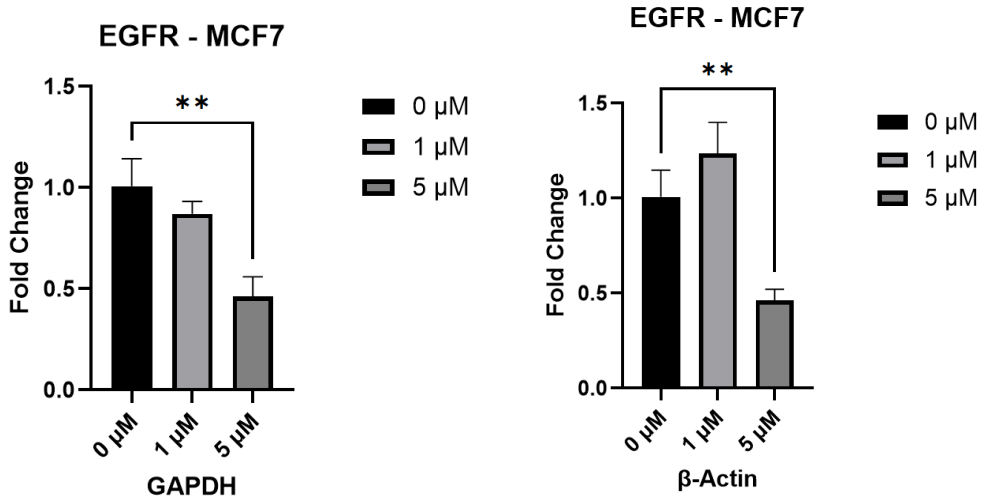

Figure 4.12. Relative expression of EGFR in MCF7 cells treated with 1 µM and 5 µM compound 5. GAPDH (left) or β-Actin (right) was used as the housekeeping gene.

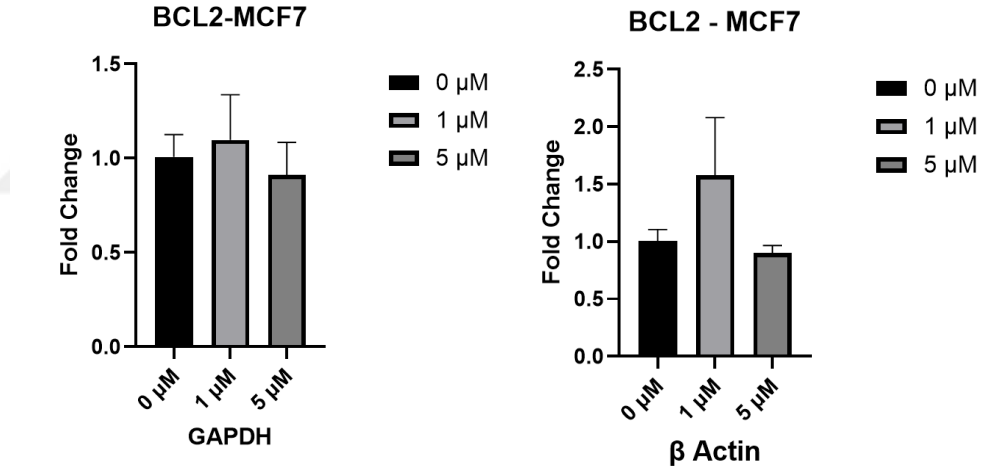

Figure 4.13. Relative expression of Bcl-2 in MCF7 cells treated with 1 µM and 5 µM doses of Compound 5. GAPDH (left) or β-Actin (right) was used as the housekeeping gene.

Interestingly, when MCF7 cells are treated with compound 5, c-MYC mRNA level increases to some extent (Figures 4.14). Recently, G4 structures on the c-MYC promoter are reported to positively regulate transcription (Esain-Garcia et. al. 2024).

Whether the observed results are due to the same reason or not needs to be analyzed extensively with more experimental replicates.

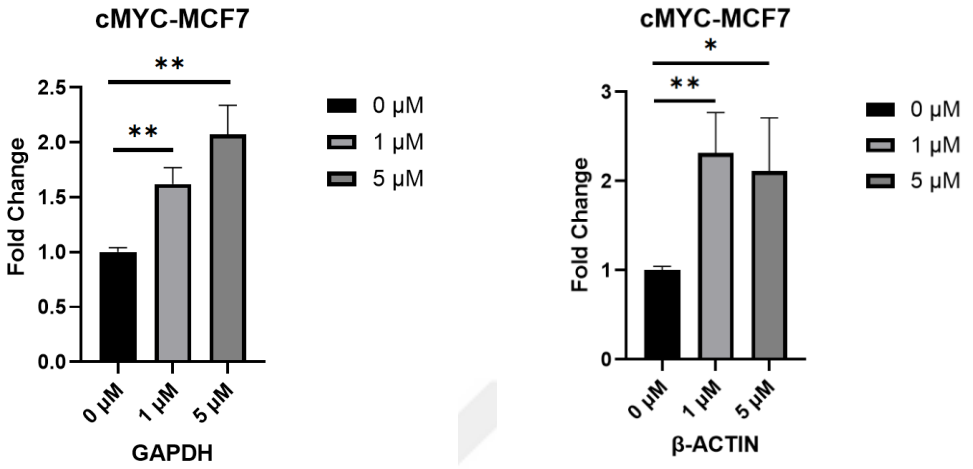

Figure 4.14. Relative expression of c-Myc in MCF7 cells treated with 1 µM and 5 µM doses of Compound 5. GAPDH (left) or β-Actin (right) was used as the housekeeping gene.

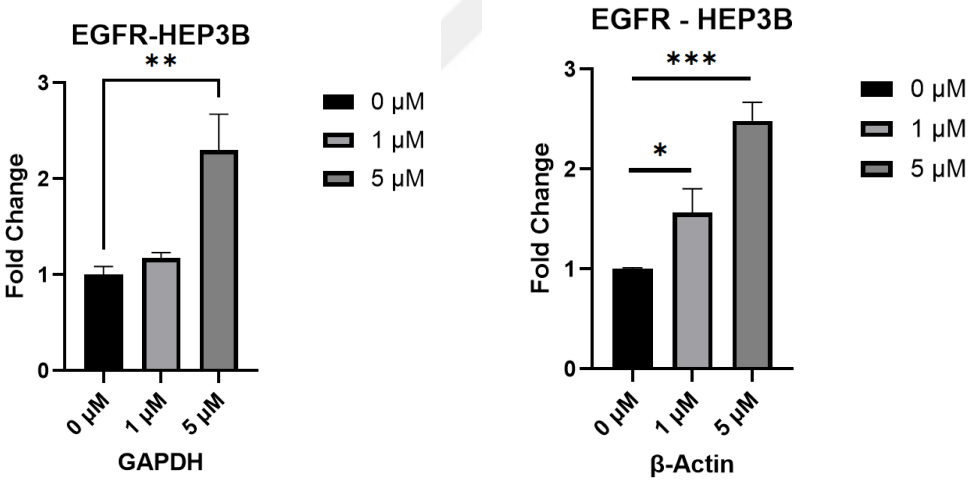

Figure 4.15. Relative expression of EGFR in Hep3B cells treated with 1 µM and 5 µM doses of Compound 5. GAPDH (left) or β-Actin (right) was used as the housekeeping gene.

When compound 5 treated HEP3B cells were analyzed, EGFR mRNA level is shown to increase (Figure 4.15). BCL2 is elevated slightly at higher doses when β- actin is used as housekeeping reference gene, however this increase is not statistically

significant when GAPDH is used as reference gene (Figure 4.16) and there was not a significant change in the expression of c-MYC (Figure 4.17).

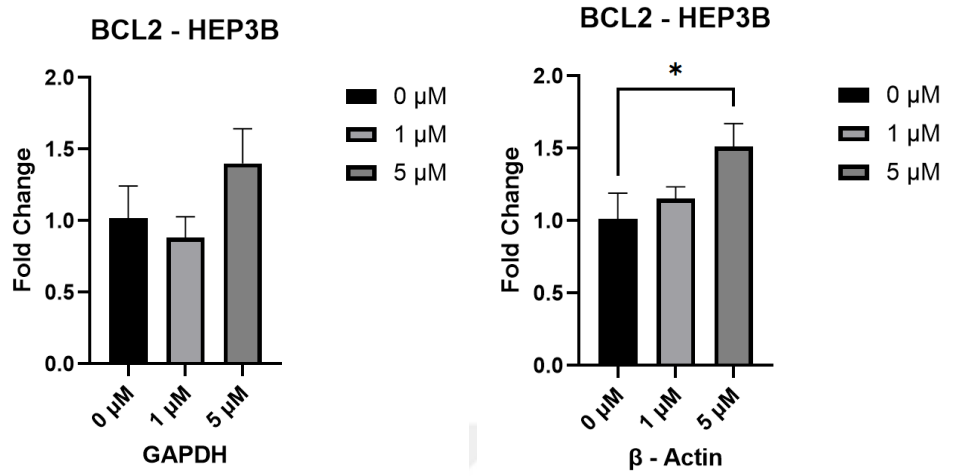

Figure 4.16. Relative expression of BCL-2 in Hep3B cells treated with 1 µM and 5 µM doses of Compound 5. GAPDH (left) or β-Actin (right) was used as the housekeeping gene.

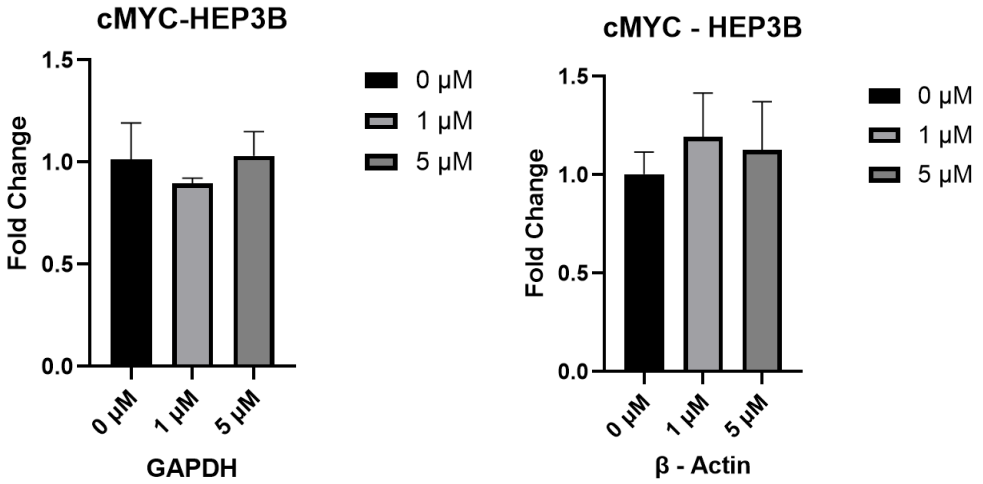

Figure 4.17. Relative expression of c-Myc in Hep3B cells treated with 1 µM and 5 µM doses of Compound 5. GAPDH (left) or β-Actin (right) was used as the housekeeping gene.

In SW480 colon cancer cells, compound 5 is treated at 5 µM dose and the relative expression of vimentin and c-MYC genes were analyzed (Figure 4.18). In both genes, treated cells displayed a significant decrease in mRNA level.

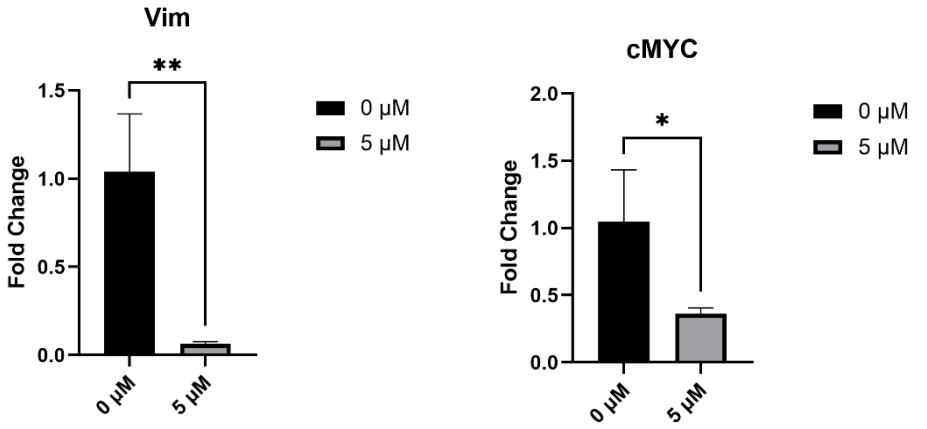

Figure 4.18. Relative expression of Vimentin and c-Myc in SW480 cells treated with 5 µM dose of Compound 5. GAPDH was used as a housekeeping gene.

4.6. Western-Blot Results

Western blot analysis was performed as stated in the method section. Analysis for the 1 µM Compound 5 treatment caused a statistically significant decrease in c-MYC protein expression in both MCF7 and SW480 cells. Interestingly, at 5 µM doses, c-MYC level is determined to be like untreated cell control. Whether higher doses lead to non-specific interaction with other nucleic acid regions needs to be determined. More experimental replicates need to be performed to verify the existing results. BCL-2 level in MCF7 cells seems to be unaffected by the given doses of compound 5.

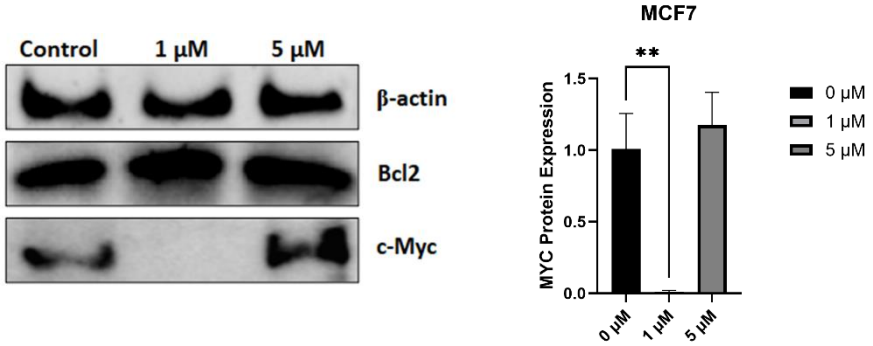

Figure 4.19. Western Blot analysis of MCF7 cells treated with compound 5 (left) and relative calculated protein expression (right). p = 0.0022.

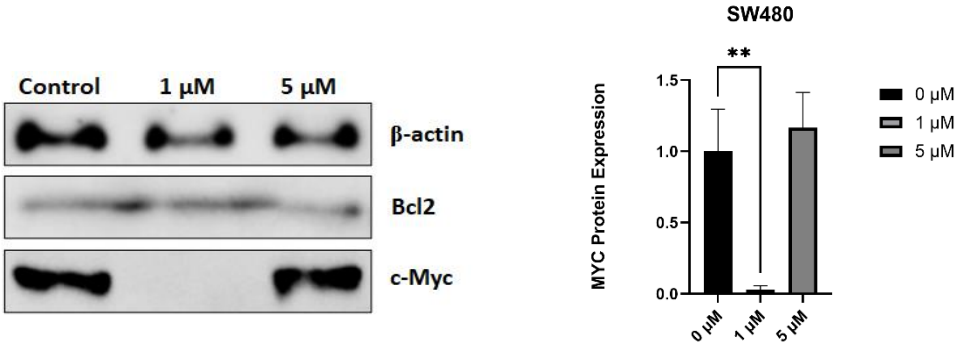

Figure 4.20. Western Blot analysis of SW480 cells treated with compound 5 (left) and relative calculated protein expression (right). p = 0.0049.

Analysis for the 1 μM Compound 5 treatment caused a statistically significant, more than 30-fold decrease in c-MYC protein expression in SW480 cells (Figure 4.20). At 5 μM doses, c-MYC level in SW480 is determined to be 22% less than untreated cell control, however this result is not statistically significant. BCL-2 level decreases in the presence of 5 μM compound 5. More data is required to assess the statistical significance of this reduction.

5. CONCLUSIONS AND RECOMMENDATIONS

5.1 Conclusions

In this thesis work, a probe for the detection of EGFR level is developed and used to measure relative levels of this receptor in human breast, colon and liver cells using fluorescence microscopy and flow cytometry techniques. MCF7 breast cancer cells have maximum fluorescence which is interpreted as high EGFR expression. For the first time in this study, BODIPY-based G-quadruplex agents are shown to reduce EGFR expression significantly in MCF7 cells but increase the expression in HEP3B. In addition, c-MYC protein level is shown to be reduced in a dose dependent manner in both SW480 and MCF7 cells, for the first time. G4 stabilizer has no effect on BCL2 protein level in MCF7 however in SW480 colon cells, 5 μM G4 stabilizer reduces the level of this protein.

It has been shown that the change in mRNA and protein level is cell specific. The cell specificity may arise from EGFR expression level, but it has to be proved with further experiments. It has been shown that mRNA level may not be directly positively correlated with protein level. Indeed, G4 stabilizer increased the mRNA level of c-MYC but protein level seems to be reduced. The result may result from promotion of transcription and inhibiting translation, the latter may be due to G4 structures on mRNA. Additionally, c-MYC expression is regulated by many other pathways. Therefore, G4 stabilizer might modulate the level of certain other gene products, indirectly the level of c-MYC can be altered in return. Experiments should be repeated with more technical replicates and additional experiments should be designed to resolve the involvement of related cellular pathways.

5.2 Recommendations

To elucidate the selectivity of the probe additional experiments are required. To understand the biological effect of BODIPY-based G4 stabilizers, proteomic analysis should be done. Although c-MYC protein level is significantly reduced by BODIPY-G4 stabilizer, current data cannot provide an explicit proof of stabilization of mRNA G4s. Extensive experimental analysis to understand the crosstalk of pathways are recommended.

6. REFERENCES

Agarwala, P., Pandey, S., & Maiti, S. (2015). The tale of RNA G-quadruplex. *Organic & Biomolecular Chemistry*, *13*(20), 5570–5585. https://doi.org/10.1039/C4OB02681K

An, F., Xin, J., Deng, C., Tan, X., Aras, O., Chen, N., Zhang, X., & Ting, R. (2021). Facile synthesis of near-infrared bodipy by donor engineering for in vivo tumor targeted dual-modal imaging. *Journal of Materials Chemistry B*, *9*(45), 9308–9315. https://doi.org/10.1039/D1TB01883C

Anisuzzaman, A., Haque, A., … D. W.-M. cancer, & 2017, undefined. (n.d.). In Vitro and In Vivo Synergistic Antitumor Activity of the Combination of BKM120 and Erlotinib in Head and Neck Cancer: Mechanism of Apoptosis and Resistance. *AACRASM Anisuzzaman, A Haque, D Wang, MA Rahman, C Zhang, Z Chen, ZG Chen, DM ShinMolecular Cancer Therapeutics, 2017•AACR*. Retrieved November 21, 2024, from https://aacrjournals.org/mct/article-abstract/16/4/729/272546

Arora, A., & Suess, B. (2011). An RNA G-quadruplex in the 3′ UTR of the proto-oncogene PIM1 represses translation. *RNA Biology*, *8*(5), 802–805. https://doi.org/10.4161/RNA.8.5.16038

Asamitsu, S., Obata, S., Yu, Z., Bando, T., Molecules, H. S.-, & 2019, undefined. (n.d.). Recent progress of targeted G-quadruplex-preferred ligands toward cancer therapy. *Mdpi.ComS Asamitsu, S Obata, Z Yu, T Bando, H SugiyamaMolecules, 2019•mdpi.Com*. Retrieved November 23, 2024, from https://www.mdpi.com/1420-3049/24/3/429

Balasubramanian, S., Hurley, L. H., & Neidle, S. (2011). Targeting G-quadruplexes in gene promoters: a novel anticancer strategy? *Nature Reviews Drug Discovery*, *10*(4), 261–275. https://doi.org/10.1038/nrd3428

Baser, A., Basar, B., Dogan, H. B., Sener, G., Ozsamur, N. G., Celik, F. S., Altves, S., & Erbas-Cakmak, S. (2023). Reprograming cancer cells by a BODIPY G-quadruplex stabiliser. *Chemical Communications*, *59*(83), 12447–12450. https://doi.org/10.1039/D3CC03453D

Bassan, E., Gualandi, A., Cozzi, P. G., & Ceroni, P. (2021). Design of BODIPY dyes as triplet photosensitizers: electronic properties tailored for solar energy conversion,

photoredox catalysis and photodynamic therapy. *Chemical Science*, *12*(19), 6607–6628. https://doi.org/10.1039/D1SC00732G

Beaudoin, J., research, J. P.-N. acids, & 2010, undefined. (n.d.). 5′-UTR G-quadruplex structures acting as translational repressors. *Nucleic Acids Research*. Retrieved November 23, 2024, from https://academic.oup.com/nar/article-abstract/38/20/7022/1302464

Benedetti, A. De, Oncogene, J. G.-, & 2004, undefined. (n.d.). eIF-4E expression and its role in malignancies and metastases. *Nature.ComA De Benedetti, JR GraffOncogene, 2004•nature.Com*. Retrieved November 22, 2024, from https://www.nature.com/articles/1207545

Bhattacharyya, D., Mirihana Arachchilage, G., & Basu, S. (2016). Metal Cations in G-Quadruplex Folding and Stability. *Frontiers in Chemistry*, *4*. https://doi.org/10.3389/fchem.2016.00038

Biffi, G., Tannahill, D., McCafferty, J., & Balasubramanian, S. (2013). Quantitative visualization of DNA G-quadruplex structures in human cells. *Nature Chemistry 2013 5:3*, *5*(3), 182–186. https://doi.org/10.1038/nchem.1548

Bochman, M. L., Paeschke, K., & Zakian, V. A. (2012). DNA secondary structures: stability and function of G-quadruplex structures. *Nature Reviews Genetics*, *13*(11), 770–780. https://doi.org/10.1038/nrg3296

Boens, N., Verbelen, B., & Dehaen, W. (2015). Postfunctionalization of the BODIPY Core: Synthesis and Spectroscopy. *European Journal of Organic Chemistry*, *2015*(30), 6577–6595. https://doi.org/10.1002/EJOC.201500682

Bonnal, S., Schaeffer, C., Créancier, L., … S. C.-J. of B., & 2003, undefined. (n.d.). A single internal ribosome entry site containing a G quartet RNA structure drives fibroblast growth factor 2 gene expression at four alternative translation initiation. *ASBMB*. Retrieved November 23, 2024, from https://www.jbc.org/article/S0021-9258(20)82974-3/fulltext

Brennan, C. M., & Steitz, J. A. (2001a). HuR and mRNA stability. *Cellular and Molecular Life Sciences*, *58*(2), 266–277. https://doi.org/10.1007/PL00000854

Brennan, C. M., & Steitz, J. A. (2001b). HuR and mRNA stability. *Cellular and Molecular Life Sciences*, *58*(2), 266–277. https://doi.org/10.1007/PL00000854

Bugaut, A., research, S. B.-N. acids, & 2012, undefined. (n.d.). 5′-UTR RNA G-quadruplexes: translation regulation and targeting. *Academic.Oup.ComA Bugaut, S*

BalasubramanianNucleic Acids Research, 2012•academic.Oup.Com. Retrieved November 23, 2024, from https://academic.oup.com/nar/article-abstract/40/11/4727/2409040

Bulut, I., Huaulmé, Q., Mirloup, A., Chávez, P., Fall, S., Hébraud, A., Méry, S., Heinrich, B., Heiser, T., Lévêque, P., & Leclerc, N. (2017). Rational Engineering of BODIPY-Bridged Trisindole Derivatives for Solar Cell Applications. *ChemSusChem*, *10*(9), 1878–1882. https://doi.org/10.1002/CSSC.201700465

Burge, S., Parkinson, G. N., Hazel, P., Todd, A. K., & Neidle, S. (2006). Quadruplex DNA: sequence, topology and structure. *Nucleic Acids Research*, *34*(19), 5402–5415. https://doi.org/10.1093/nar/gkl655

Capra, J. A., Paeschke, K., Singh, M., & Zakian, V. A. (2010). G-quadruplex DNA sequences are evolutionarily conserved and associated with distinct genomic features in Saccharomyces cerevisiae. *PLoS Computational Biology*, *6*(7), 9. https://doi.org/10.1371/JOURNAL.PCBI.1000861

Chalupníková, K., Lattmann, S., … N. S.-J. of B., & 2008, undefined. (n.d.). Recruitment of the RNA helicase RHAU to stress granules via a unique RNA-binding domain. *ASBMB*. Retrieved November 22, 2024, from https://www.jbc.org/article/S0021-9258(20)63342-7/fulltext

Chambers, V., Marsico, G., … J. B.-N., & 2015, undefined. (n.d.). High-throughput sequencing of DNA G-quadruplex structures in the human genome. *Nature.ComVS Chambers, G Marsico, JM Boutell, M Di Antonio, GP Smith, S BalasubramanianNature Biotechnology, 2015•nature.Com*. Retrieved November 23, 2024, from https://www.nature.com/articles/nbt.3295

Chen, M., Tippana, R., Demeshkina, N., Nature, P. M.-, & 2018, undefined. (n.d.). Structural basis of G-quadruplex unfolding by the DEAH/RHA helicase DHX36. *Nature.ComMC Chen, R Tippana, NA Demeshkina, P Murat, S Balasubramanian, S MyongNature, 2018•nature.Com*. Retrieved November 24, 2024, from https://www.nature.com/articles/s41586-018-0209-9

Chen, Y., Zhao, J., Guo, H., & Xie, L. (2012). Geometry relaxation-induced large stokes shift in red-emitting borondipyrromethenes (BODIPY) and applications in fluorescent thiol probes. *Journal of Organic Chemistry*, *77*(5), 2192–2206. https://doi.org/10.1021/JO202215X

Chi, C. C., Huang, Y. J., & Chen, C. T. (2012). Synthesis and spectroscopic characterization of dual absorption BODIPY type dyes and their light harvesting application in polymer-based bulk hetrojunction organic photovoltaics. *Journal of the Chinese Chemical Society*, *59*(3), 305–316. https://doi.org/10.1002/JCCS.201100612

Cogoi, S., research, L. X.-N. acids, & 2006, undefined. (n.d.). G-quadruplex formation within the promoter of the KRAS proto-oncogene and its effect on transcription. *Academic.Oup.ComS Cogoi, LE XodoNucleic Acids Research, 2006•academic.Oup.Com*. Retrieved November 23, 2024, from https://academic.oup.com/nar/article-abstract/34/9/2536/2401687

Collie, G., Reviews, G. P.-C. S., & 2011, undefined. (n.d.). The application of DNA and RNA G-quadruplexes to therapeutic medicines. *Pubs.Rsc.OrgGW Collie, GN ParkinsonChemical Society Reviews, 2011•pubs.Rsc.Org*. Retrieved November 24, 2024, from https://pubs.rsc.org/en/content/articlehtml/2011/cs/c1cs15067g

Conlon, E., Lu, L., Sharma, A., Yamazaki, T., elife, T. T.-, & 2016, undefined. (n.d.). The C9ORF72 GGGGCC expansion forms RNA G-quadruplex inclusions and sequesters hnRNP H to disrupt splicing in ALS brains. *Elifesciences.OrgEG Conlon, L Lu, A Sharma, T Yamazaki, T Tang, NA Shneider, JL Manleyelife, 2016•elifesciences.Org*. Retrieved November 22, 2024, from https://elifesciences.org/articles/17820

Dexheimer, T. S., Sun, D., & Hurley, L. H. (2006). Deconvoluting the structural and drug-recognition complexity of the G-quadruplex-forming region upstream of the bcl-2 P1 promoter. *Journal of the American Chemical Society*, *128*(16), 5404–5415. https://doi.org/10.1021/JA0563861

Di Antonio, M., Rodriguez, R., & Balasubramanian, S. (2012). Experimental approaches to identify cellular G-quadruplex structures and functions. *Methods (San Diego, Calif.)*, *57*(1), 84–92. https://doi.org/10.1016/J.YMETH.2012.01.008

Eddy, J., research, N. M.-N. acids, & 2006, undefined. (n.d.). Gene function correlates with potential for G4 DNA formation in the human genome. *Academic.Oup.ComJ Eddy, N MaizelsNucleic Acids Research, 2006•academic.Oup.Com*. Retrieved November 21, 2024, from https://academic.oup.com/nar/article-abstract/34/14/3887/3091630

Fan, X. C., & Steitz, J. A. (1998). Overexpression... - Google Akademik. (n.d.). Retrieved November 22, 2024, from https://scholar.google.com/scholar?hl=tr&as_sdt=0%2C5&q=Fan%2C+X.+C.%2C+%26+Steitz%2C+J.+A.+%281998%29.+Overexpression+of+HuR%2C+a+nuclear-cytoplasmic+shuttling+protein%2C+increases+the+in+vivo+stability+of+ARE-containing+mRNAs.+The+EMBO+Journal%2C+17%2812%29%2C+3448%E2%80%933460.&btnG=

Figueiredo, J., Mergny, J.-L., & Cruz, C. (2024). G-quadruplex ligands in cancer therapy: Progress, challenges, and clinical perspectives. *Life Sciences*, *340*, 122481. https://doi.org/10.1016/j.lfs.2024.122481

Gavis, E., Nature, R. L.-, & 1994, undefined. (n.d.). Translational regulation of nanos by RNA localization. *Nature.ComER Gavis, R LehmannNature, 1994•nature.Com*. Retrieved November 22, 2024, from https://www.nature.com/articles/369315a0

Gomez, D., Guédin, A., Mergny, J.-L., Salles, B., Riou, J.-F., Teulade-Fichou, M.-P., & Calsou, P. (2010). A G-quadruplex structure within the 5′-UTR of TRF2 mRNA represses translation in human cells. *Nucleic Acids Research*, *38*(20), 7187–7198. https://doi.org/10.1093/nar/gkq563

Hänsel-Hertsch, R., Di Antonio, M., & Balasubramanian, S. (2017). DNA G-quadruplexes in the human genome: detection, functions and therapeutic potential. *Nature Reviews Molecular Cell Biology*, *18*(5), 279–284. https://doi.org/10.1038/nrm.2017.3

Hardin, C. C., Corregan, M., Brown, B. A., & Frederick, L. N. (1993). Cytosine—Cytosine+ Base Pairing Stabilizes DNA Quadruplexes and Cytosine Methylation Greatly Enhances the Effect. *Biochemistry*, *32*(22), 5870–5880. https://doi.org/10.1021/BI00073A021

Hattori, S., Ohkubo, K., Urano, Y., Sunahara, H., Nagano, T., Wada, Y., Tkachenko, N. V., Lemmetyinen, H., & Fukuzumi, S. (2005). Charge separation in a nonfluorescent donor-acceptor dyad derived from boron dipyrromethene dye, leading to photocurrent generation. *Journal of Physical Chemistry B*, *109*(32), 15368–15375. https://doi.org/10.1021/JP050952X

Hazel, P., Huppert, J., Balasubramanian, S., & Neidle, S. (2004). Loop-length-dependent folding of G-quadruplexes. *Journal of the American Chemical Society*, *126*(50), 16405–16415. https://doi.org/10.1021/JA045154J

Hentze, M. W., & Kühn, L. C. (1996). Molecular control of vertebrate iron metabolism: mRNA-based regulatory circuits operated by iron, nitric oxide, and oxidative stress. *Proceedings of the National Academy of Sciences*, *93*(16), 8175–8182. https://doi.org/10.1073/pnas.93.16.8175

Hentze, M. W., Rouault, T. A., Caughman, S. W., Dancis, A., Harford, J. B., & Klausner, R. D. (1987). A cis-acting element is necessary and sufficient for translational regulation of human ferritin expression in response to iron. *Proceedings of the National Academy of Sciences of the United States of America*, *84*(19), 6730–6734. https://doi.org/10.1073/PNAS.84.19.6730

Hershman, S. G., Chen, Q., Lee, J. Y., Kozak, M. L., Yue, P., Wang, L.-S., & Johnson, F. B. (2008). Genomic distribution and functional analyses of potential G-quadruplex-forming sequences in Saccharomyces cerevisiae. *Nucleic Acids Research*, *36*(1), 144–156. https://doi.org/10.1093/nar/gkm986

Hirte, H., Oza, A., Swenerton, K., Ellard, S., … R. G.-G., & 2010, undefined. (n.d.). A phase II study of erlotinib (OSI-774) given in combination with carboplatin in patients with recurrent epithelial ovarian cancer (NCIC CTG IND. 149). *ElsevierH Hirte, A Oza, K Swenerton, SL Ellard, R Grimshaw, B Fisher, M Tsao, L SeymourGynecologic Oncology, 2010•Elsevier*. Retrieved November 21, 2024, from https://www.sciencedirect.com/science/article/pii/S0090825810003616

Huang, H., Zhang, J., Harvey, S. E., Hu, X., & Cheng, C. (2017). RNA G-quadruplex secondary structure promotes alternative splicing via the RNA-binding protein hnRNPF. *Genes & Development*, *31*(22), 2296–2309. https://doi.org/10.1101/GAD.305862.117

Huppert, J. L., & Balasubramanian, S. (2005). Prevalence of quadruplexes in the human genome. *Nucleic Acids Research*, *33*(9), 2908–2916. https://doi.org/10.1093/nar/gki609

Huppert, J. L., & Balasubramanian, S. (2007). G-quadruplexes in promoters throughout the human genome. *Nucleic Acids Research*, *35*(2), 406–413. https://doi.org/10.1093/NAR/GKL1057

Huppert, J., research, S. B.-N. acids, & 2005, undefined. (n.d.). Prevalence of quadruplexes in the human genome. *Academic.Oup.ComJL Huppert, S BalasubramanianNucleic Acids Research, 2005•academic.Oup.Com*. Retrieved

November 23, 2024, from https://academic.oup.com/nar/article-abstract/33/9/2908/2401500

Izbicka, E., Wheelhouse, R., Raymond, E., research, K. D.-C., & 1999, undefined. (n.d.). Effects of cationic porphyrins as G-quadruplex interactive agents in human tumor cells. *AACRE Izbicka, RT Wheelhouse, E Raymond, KK Davidson, RA Lawrence, D Sun, BE WindleCancer Research, 1999•AACR*. Retrieved November 23, 2024, from https://aacrjournals.org/cancerres/article-abstract/59/3/639/505759

Ji, J., Zhou, H., A, H. K.-J. of M. C., & 2018, undefined. (n.d.). Rational design criteria for D–π–A structured organic and porphyrin sensitizers for highly efficient dye-sensitized solar cells. *Pubs.Rsc.OrgJM Ji, H Zhou, HK KimJournal of Materials Chemistry A, 2018•pubs.Rsc.Org*. Retrieved November 22, 2024, from https://pubs.rsc.org/en/content/articlehtml/2018/ta/c8ta02281j

Joachimi, A., Benz, A., & Hartig, J. S. (2009). A comparison of DNA and RNA quadruplex structures and stabilities. *Bioorganic & Medicinal Chemistry*, *17*(19), 6811–6815. https://doi.org/10.1016/j.bmc.2009.08.043

Kang, H., & Schuman, E. M. (1996). A requirement for local protein synthesis in neurotrophin-induced hippocampal synaptic plasticity. *Science*, *273*(5280), 1402–1406. https://doi.org/10.1126/SCIENCE.273.5280.1402

Kobayashi, H., Ogawa, M., Alford, R., Choyke, P. L., & Urano, Y. (2010). New strategies for fluorescent probe design in medical diagnostic imaging. *Chemical Reviews*, *110*(5), 2620–2640. https://doi.org/10.1021/CR900263J

Kolb, H., Finn, M., Edition, K. S.-C. I., & 2001, undefined. (2001). Click chemistry: diverse chemical function from a few good reactions. *Wiley Online LibraryHC Kolb, MG Finn, KB SharplessAngewandte Chemie International Edition, 2001•Wiley Online Library*. https://onlinelibrary.wiley.com/doi/abs/10.1002/1521-3773(20010601)40:11%3C2004::aid-anie2004%3E3.0.co;2-5

Kumari, S., Bugaut, A., … J. H.-N. chemical, & 2007, undefined. (n.d.). An RNA G-quadruplex in the 5′ UTR of the NRAS proto-oncogene modulates translation. *Nature.ComS Kumari, A Bugaut, JL Huppert, S BalasubramanianNature Chemical Biology, 2007•nature.Com*. Retrieved November 23, 2024, from https://www.nature.com/articles/nchembio864

Lee, R., Feinbaum, R., cell, V. A.-, & 1993, undefined. (n.d.). The C. elegans heterochronic gene lin-4 encodes small RNAs with antisense complementarity to

lin-14. *Cell.ComRC Lee, RL Feinbaum, V Ambroscell, 1993•cell.Com*. Retrieved November 22, 2024, from https://www.cell.com/cell/pdf/0092-8674(93)90529-Y.pdf

Lindquist, S. (1986). The heat-shock response. *Annual Review of Biochemistry*, *55*, 1151–1191. https://doi.org/10.1146/annurev.bi.55.070186.005443

Liu, X., Chi, W., Qiao, Q., Kokate, S. V., Cabrera, E. P., Xu, Z., Liu, X., & Chang, Y. T. (2020). Molecular Mechanism of Viscosity Sensitivity in BODIPY Rotors and Application to Motion-Based Fluorescent Sensors. *ACS Sensors*, *5*(3), 731–739. https://doi.org/10.1021/ACSSENSORS.9B01951

Loudet, A., & Burgess, K. (2007). BODIPY dyes and their derivatives: Syntheses and spectroscopic properties. *Chemical Reviews*, *107*(11), 4891–4932. https://doi.org/10.1021/CR078381N

Magde, D., Rojas, G..E., Seybold, P. 1999, Solvent Dependence of the Fluorescence Lifetimes of Xanthene Dyes, Photochemistry Photobiology, 70, 737-44.

Marcel, V., Tran, P., Sagne, C., … G. M.-P.-, & 2011, undefined. (n.d.). G-quadruplex structures in TP53 intron 3: role in alternative splicing and in production of p53 mRNA isoforms. *Academic.Oup.ComV Marcel, PLT Tran, C Sagne, G Martel-Planche, L Vaslin, MP Teulade-Fichou, J HallCarcinogenesis, 2011•academic.Oup.Com*. Retrieved November 23, 2024, from https://academic.oup.com/carcin/article-abstract/32/3/271/2463608

medicine, M. M.-T. control in biology and, & 2007, undefined. (n.d.). Origins and principles of translational control. *Cir.Nii.Ac.Jp*. Retrieved November 22, 2024, from https://cir.nii.ac.jp/crid/1572543026100897792

Mendoza, O., Bourdoncle, A., research, J. B.-… acids, & 2016, undefined. (n.d.). G-quadruplexes and helicases. *Academic.Oup.ComO Mendoza, A Bourdoncle, JB Boulé, RM Brosh Jr, JL MergnyNucleic Acids Research, 2016•academic.Oup.Com*. Retrieved November 24, 2024, from https://academic.oup.com/nar/article-abstract/44/5/1989/2465419

Merkes, J., Ostlender, T., Wang, F., Chemistry, F. K.-… J. of, & 2021, undefined. (n.d.). Tuning the optical properties of BODIPY dyes by N-rich heterocycle conjugation using a combined synthesis and computational approach. *Pubs.Rsc.OrgJM Merkes, T Ostlender, F Wang, F Kiessling, H Sun, S BanalaNew Journal of Chemistry,*

2021•pubs.Rsc.Org. Retrieved November 22, 2024, from https://pubs.rsc.org/en/content/articlehtml/2021/nj/d1nj01847g

Mikulchyk, T., Karuthedath, S., De Castro, C. S. P., Buglak, A. A., Sheehan, A., Wieder, A., Laquai, F., Naydenova, I., & Filatov, M. A. (2022). Charge transfer mediated triplet excited state formation in donor–acceptor–donor BODIPY: Application for recording of holographic structures in photopolymerizable glass. *Journal of Materials Chemistry C*, *10*(32), 11588–11597. https://doi.org/10.1039/D2TC02263J

Moreno, J., Radford, H., Peretti, D., Steinert, J., Nature, N. V.-, & 2012, undefined. (n.d.). Sustained translational repression by eIF2α-P mediates prion neurodegeneration. *Nature.ComJA Moreno, H Radford, D Peretti, JR Steinert, N Verity, MG Martin, M Halliday, J MorganNature, 2012•nature.Com*. Retrieved November 22, 2024, from https://www.nature.com/articles/nature11058

Moyer, J., Barbacci, E., Iwata, K., Arnold, L., research, B. B.-C., & 1997, undefined. (n.d.). Induction of apoptosis and cell cycle arrest by CP-358,774, an inhibitor of epidermal growth factor receptor tyrosine kinase. *AACRJD Moyer, EG Barbacci, KK Iwata, L Arnold, B Boman, A Cunningham, C DiOrio, J DotyCancer Research, 1997•AACR*. Retrieved November 21, 2024, from https://aacrjournals.org/cancerres/article-abstract/57/21/4838/503721

Müller, S., & Rodriguez, R. (2014). G-quadruplex interacting small molecules and drugs: From bench toward bedside. *Expert Review of Clinical Pharmacology*, *7*(5), 663–679. https://doi.org/10.1586/17512433.2014.945909

Müller, S., Sanders, D., Antonio, M. Di, … S. M.-O. &, & 2012, undefined. (n.d.). Pyridostatin analogues promote telomere dysfunction and long-term growth inhibition in human cancer cells. *Pubs.Rsc.OrgS Müller, DA Sanders, M Di Antonio, S Matsis, JF Riou, R Rodriguez, S BalasubramanianOrganic & Biomolecular Chemistry, 2012•pubs.Rsc.Org*. Retrieved November 23, 2024, from https://pubs.rsc.org/en/content/articlehtml/2012/ob/c2ob25830g

Nakken, S., Rognes, T., research, E. H.-N. acids, & 2009, undefined. (n.d.). The disruptive positions in human G-quadruplex motifs are less polymorphic and more conserved than their neutral counterparts. *Academic.Oup.ComS Nakken, T Rognes, E HovigNucleic Acids Research, 2009•academic.Oup.Com*. Retrieved November 21, 2024, from https://academic.oup.com/nar/article-abstract/37/17/5749/1079367

Neidle, S. (2017). Quadruplex nucleic acids as targets for anticancer therapeutics. *Nature Reviews Chemistry 2017 1:5*, *1*(5), 1–10. https://doi.org/10.1038/s41570-017-0041

Neidle, S., biology, G. P.-C. opinion in structural, & 2003, undefined. (n.d.). The structure of telomeric DNA. *ElsevierS Neidle, GN ParkinsonCurrent Opinion in Structural Biology, 2003•Elsevier*. Retrieved November 23, 2024, from https://www.sciencedirect.com/science/article/pii/S0959440X03000721

Niu, K., Zhang, X., Song, Q., Molecular, Q. F.-I. J. of, & 2022, undefined. (n.d.). G-Quadruplex Regulation of VEGFA mRNA Translation by RBM4. *Mdpi.ComK Niu, X Zhang, Q Song, Q FengInternational Journal of Molecular Sciences, 2022•mdpi.Com*. Retrieved November 24, 2024, from https://www.mdpi.com/1422-0067/23/2/743

O'Hagan, M. P., Morales, J. C., & Galan, M. C. (2019). Binding and Beyond: What Else Can G-Quadruplex Ligands Do? *European Journal of Organic Chemistry*, *2019*(31–32), 4995–5017. https://doi.org/10.1002/EJOC.201900692

Perrone, R., Lavezzo, E., Riello, E., Manganelli, R., reports, G. P.-S., & 2017, undefined. (n.d.). Mapping and characterization of G-quadruplexes in Mycobacterium tuberculosis gene promoter regions. *Nature.ComR Perrone, E Lavezzo, E Riello, R Manganelli, G Palù, S Toppo, R Provvedi, SN RichterScientific Reports, 2017•nature.Com*. Retrieved November 23, 2024, from https://www.nature.com/articles/s41598-017-05867-z

Rawal, P., Kummarasetti, V., … J. R.-G., & 2006, undefined. (n.d.). Genome-wide prediction of G4 DNA as regulatory motifs: role in Escherichia coli global regulation. *Genome.Cshlp.OrgP Rawal, VBR Kummarasetti, J Ravindran, N Kumar, K Halder, R Sharma, M MukerjiGenome Research, 2006•genome.Cshlp.Org*. Retrieved November 21, 2024, from https://genome.cshlp.org/content/16/5/644.short

Richl, T., Kuper, J., & Kisker, C. (2024). G-quadruplex-mediated genomic instability drives SNVs in cancer. *Nucleic Acids Research*, *52*(5), 2198–2211. https://doi.org/10.1093/nar/gkae098

Rigo, R., Palumbo, M., (BBA)-General, C. S.-B. et B. A., & 2017, undefined. (n.d.). G-quadruplexes in human promoters: A challenge for therapeutic applications. *ElsevierR Rigo, M Palumbo, C SissiBiochimica et Biophysica Acta (BBA)-General*

Subjects, 2017•Elsevier. Retrieved November 24, 2024, from https://www.sciencedirect.com/science/article/pii/S0304416516305189

Robinow, S., Campos, A. R., Yao, K. M., & White, K. (1988). The elav gene product of Drosophila, required in neurons, has three RNP consensus motifs. *Science (New York, N.Y.)*, *242*(4885), 1570–1572. https://doi.org/10.1126/SCIENCE.3144044

Rouleau, S. G., Garant, J. M., Bolduc, F., Bisaillon, M., & Perreault, J. P. (2018). G-Quadruplexes influence pri-microRNA processing. *RNA Biology*, *15*(2), 198–206. https://doi.org/10.1080/15476286.2017.1405211

Sansalone, L., Tang, S., Garcia-Amorós, J., Zhang, Y., Nonell, S., Baker, J. D., Captain, B., & Raymo, F. M. (2018). A Photoactivatable Far-Red/Near-Infrared BODIPY To Monitor Cellular Dynamics in Vivo. *ACS Sensors*, *3*(7), 1347–1353. https://doi.org/10.1021/acssensors.8b00262

Sarkies, P., Reams, C., Simpson, L., cell, J. S.-M., & 2010, undefined. (n.d.). Epigenetic instability due to defective replication of structured DNA. *Cell.ComP Sarkies, C Reams, LJ Simpson, JE SaleMolecular Cell, 2010•cell.Com*. Retrieved November 23, 2024, from https://www.cell.com/molecular-cell/fulltext/S1097-2765(10)00847-6

Schaeffer, C., Bardoni, B., Mandel, J. L., Ehresmann, B., Ehresmann, C., & Moine, H. (2001). The fragile X mental retardation protein binds specifically to its mRNA via a purine quartet motif. *EMBO Journal*, *20*(17), 4803–4813. https://doi.org/10.1093/EMBOJ/20.17.4803

Schiavone, D., Guilbaud, G., Murat, P., Papadopoulou, C., Sarkies, P., Prioleau, M., Balasubramanian, S., & Sale, J. E. (2014). Determinants of G quadruplex-induced epigenetic instability in REV 1-deficient cells . *The EMBO Journal*, *33*(21), 2507–2520. https://doi.org/10.15252/EMBJ.201488398

Siddiqui-Jain, A., Grand, C. L., Bearss, D. J., & Hurley, L. H. (2002). Direct evidence for a G-quadruplex in a promoter region and its targeting with a small molecule to repress c-MYC transcription. *Proceedings of the National Academy of Sciences of the United States of America*, *99*(18), 11593–11598. https://doi.org/10.1073/PNAS.182256799

Simone, R., Fratta, P., Neidle, S., Parkinson, G., letters, A. I.-F., & 2015, undefined. (n.d.). G-quadruplexes: Emerging roles in neurodegenerative diseases and the non-coding transcriptome. *ElsevierR Simone, P Fratta, S Neidle, GN Parkinson, AM*

IsaacsFEBS Letters, 2015•Elsevier. Retrieved November 23, 2024, from https://www.sciencedirect.com/science/article/pii/S0014579315003567

Smestad, J. A., & Maher, L. J. (2015). Relationships between putative G-quadruplex-forming sequences, RecQ helicases, and transcription. *BMC Medical Genetics*, *16*(1). https://doi.org/10.1186/S12881-015-0236-4

Su, Z., Zhang, Y., Gendron, T. F., Bauer, P. O., Chew, J., Yang, W. Y., Fostvedt, E., Jansen-West, K., Belzil, V. V., Desaro, P., Johnston, A., Overstreet, K., Oh, S. Y., Todd, P. K., Berry, J. D., Cudkowicz, M. E., Boeve, B. F., Dickson, D., Floeter, M. K., … Disney, M. D. (2014). Discovery of a Biomarker and Lead Small Molecules to Target r(GGGGCC)-Associated Defects in c9FTD/ALS. *Neuron*, *83*(5), 1043–1050. https://doi.org/10.1016/j.neuron.2014.07.041

Subramanian, M., Rage, F., Tabet, R., Flatter, E., Mandel, J. L., & Moine, H. (2011). G-quadruplex RNA structure as a signal for neurite mRNA targeting. *EMBO Reports*, *12*(7), 697–704. https://doi.org/10.1038/EMBOR.2011.76

Sun, D., Guo, K., Rusche, J., research, L. H.-N. acids, & 2005, undefined. (n.d.). Facilitation of a structural transition in the polypurine/polypyrimidine tract within the proximal promoter region of the human VEGF gene by the presence of potassium. *Academic.Oup.ComD Sun, K Guo, JJ Rusche, LH HurleyNucleic Acids Research, 2005•academic.Oup.Com*. Retrieved November 23, 2024, from https://academic.oup.com/nar/article-abstract/33/18/6070/2401355

Todd, A., Johnston, M., research, S. N.-N. acids, & 2005, undefined. (n.d.). Highly prevalent putative quadruplex sequence motifs in human DNA. *Academic.Oup.ComAK Todd, M Johnston, S NeidleNucleic Acids Research, 2005•academic.Oup.Com*. Retrieved November 21, 2024, from https://academic.oup.com/nar/article-abstract/33/9/2901/2401387

Tram, K., Yan, H., Jenkins, H., Vassiliev, S., Pigments, D. B.-D. and, & 2009, undefined. (n.d.). The synthesis and crystal structure of unsubstituted 4, 4-difluoro-4-bora-3a, 4a-diaza-s-indacene (BODIPY). *ElsevierK Tram, H Yan, HA Jenkins, S Vassiliev, D BruceDyes and Pigments, 2009•Elsevier*. Retrieved November 22, 2024, from https://www.sciencedirect.com/science/article/pii/S0143720809000448

Treibs, A., & Kreuzer, F. (1968). Difluorboryl-Komplexe von Di- und Tripyrrylmethenen. *Justus Liebigs Annalen Der Chemie*, *718*(1), 208–223. https://doi.org/10.1002/jlac.19687180119

Umasekhar, B., Ganapathi, E., Transactions, T. C.-…, & 2015, undefined. (n.d.). Synthesis, structure, and spectral, electrochemical and fluoride sensing properties of meso-pyrrolyl boron dipyrromethene. *Pubs.Rsc.OrgB Umasekhar, E Ganapathi, T Chatterjee, M RavikanthDalton Transactions, 2015•pubs.Rsc.Org*. Retrieved November 22, 2024, from https://pubs.rsc.org/en/content/articlehtml/2015/dt/c5dt02634b

Uyar, B., Ozsamur, N. G., Celik, F. S., Ozbayram, I., & Erbas-Cakmak, S. (2023). Downregulation of gene expression in hypoxic cancer cells by an activatable G-quadruplex stabiliser. *Chemical Communications*, *59*(16), 2247–2250. https://doi.org/10.1039/D2CC06347F

Valentin-Vega, Y. A., Wang, Y.-D., Parker, M., Patmore, D. M., Kanagaraj, A., Moore, J., Rusch, M., Finkelstein, D., Ellison, D. W., Gilbertson, R. J., Zhang, J., Kim, H. J., & Taylor, J. P. (2016). Cancer-associated DDX3X mutations drive stress granule assembly and impair global translation. *Scientific Reports*, *6*(1), 25996. https://doi.org/10.1038/srep25996

Varshney, D., Spiegel, J., Zyner, K., Tannahill, D., & Balasubramanian, S. (2020). The regulation and functions of DNA and RNA G-quadruplexes. *Nature Reviews Molecular Cell Biology*, *21*(8), 459–474. https://doi.org/10.1038/s41580-020-0236-x

Watson, J. D., & Crick, F. H. C. (1953). Molecular Structure of Nucleic Acids: A Structure for Deoxyribose Nucleic Acid. *Nature 1953 171:4356*, *171*(4356), 737–738. https://doi.org/10.1038/171737a0

Wek, R., Jiang, H., Society, T. A.-B., & 2006, undefined. (n.d.). Coping with stress: eIF2 kinases and translational control. *Portlandpress.ComRC Wek, HY Jiang, TG AnthonyBiochemical Society Transactions, 2006•portlandpress.Com*. Retrieved November 22, 2024, from https://portlandpress.com/biochemsoctrans/article-abstract/34/1/7/64152

Wieland, M., biology, J. H.-C. &, & 2007, undefined. (n.d.). RNA quadruplex-based modulation of gene expression. *Cell.ComM Wieland, JS HartigChemistry & Biology, 2007•cell.Com*. Retrieved November 23, 2024, from https://www.cell.com/ccbio/fulltext/S1074-5521(07)00210-4

Xu, H., Di Antonio, M., McKinney, S., Mathew, V., Ho, B., O'Neil, N. J., Santos, N. Dos, Silvester, J., Wei, V., Garcia, J., Kabeer, F., Lai, D., Soriano, P., Banáth, J.,

Chiu, D. S., Yap, D., Le, D. D., Ye, F. B., Zhang, A., … Aparicio, S. (2017). CX-5461 is a DNA G-quadruplex stabilizer with selective lethality in BRCA1/2 deficient tumours. *Nature Communications 2017 8:1*, *8*(1), 1–18. https://doi.org/10.1038/ncomms14432

Yadav, I. S., & Misra, R. (2023). Design, synthesis and functionalization of BODIPY dyes: applications in dye-sensitized solar cells (DSSCs) and photodynamic therapy (PDT). *Journal of Materials Chemistry C*, *11*(26), 8688–8723. https://doi.org/10.1039/D3TC00171G

Zhao, J., Wu, W., Sun, J., Reviews, S. G.-C. S., & 2013, undefined. (n.d.). Triplet photosensitizers: from molecular design to applications. *Pubs.Rsc.OrgJ Zhao, W Wu, J Sun, S GuoChemical Society Reviews, 2013•pubs.Rsc.Org*. Retrieved November 21, 2024, from https://pubs.rsc.org/en/content/articlehtml/2013/cs/c3cs35531d

Zhu, S., Bi, J., Vegesna, G., Zhang, J., … F. L.-R., & 2013, undefined. (n.d.). Functionalization of BODIPY dyes at 2, 6-positions through formyl groups. *Pubs.Rsc.OrgS Zhu, J Bi, G Vegesna, J Zhang, FT Luo, L Valenzano, H LiuRSC Advances, 2013•pubs.Rsc.Org*. Retrieved November 22, 2024, from https://pubs.rsc.org/en/content/articlehtml/2013/ra/c3ra22610g

APPENDIX

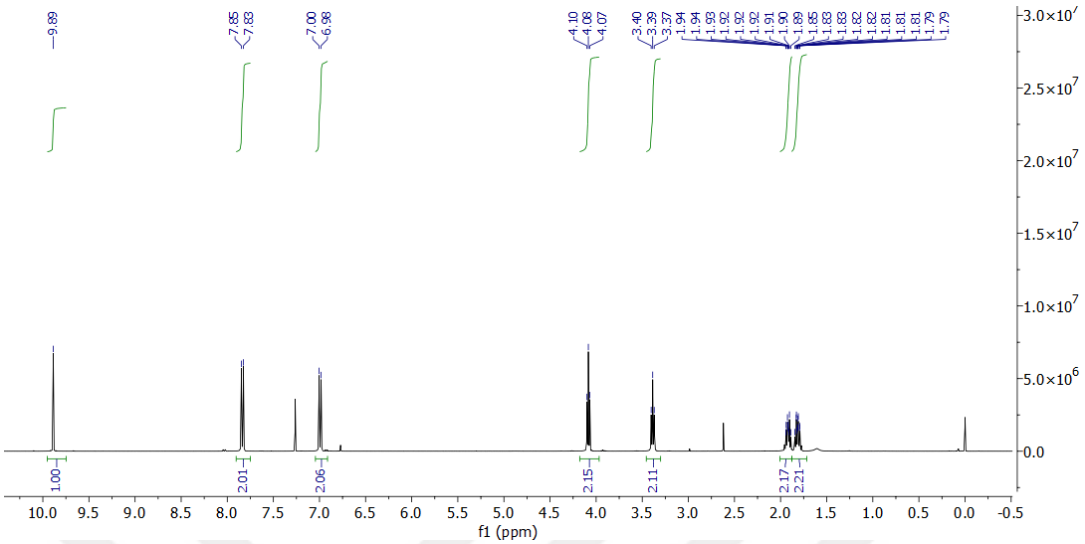

ANNEX-1 ^{1}H NMR Spcetrum of Compound 2 ($CDCl_3$, 400 MHz)

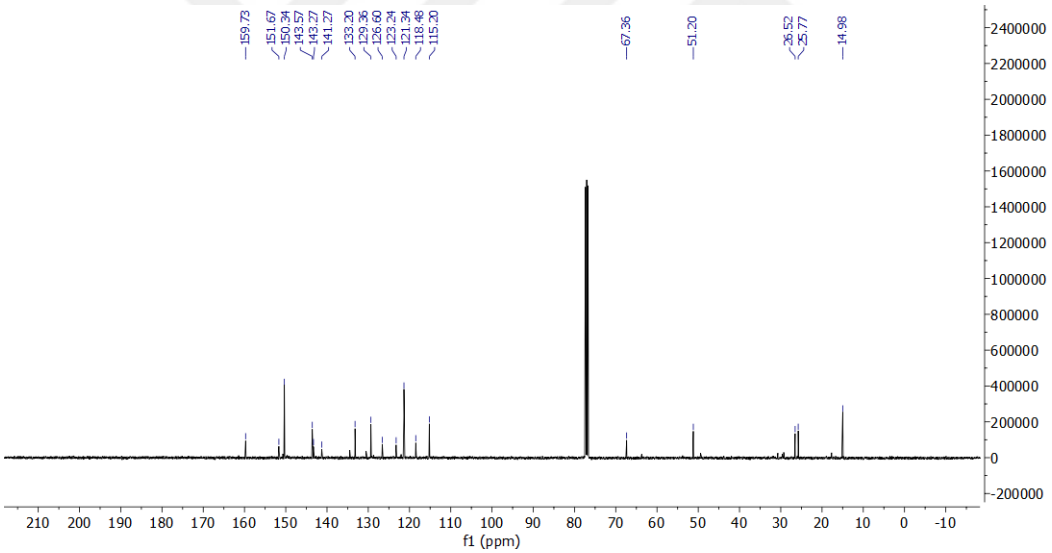

ANNEX-2 ^{13}C NMR Spcetrum of Compound 4 ($CDCl_3$, 400 MHz)

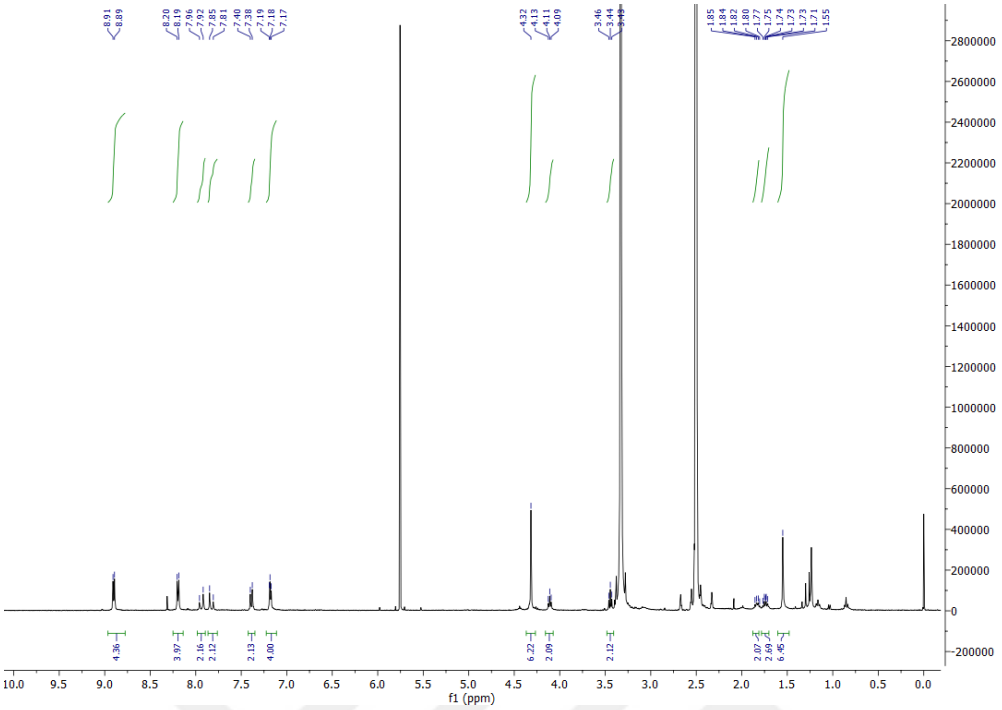

ANNEX-3 ^{1}H NMR Spcetrum of Compound 5 (DMSO-*d*, 400 MHz)

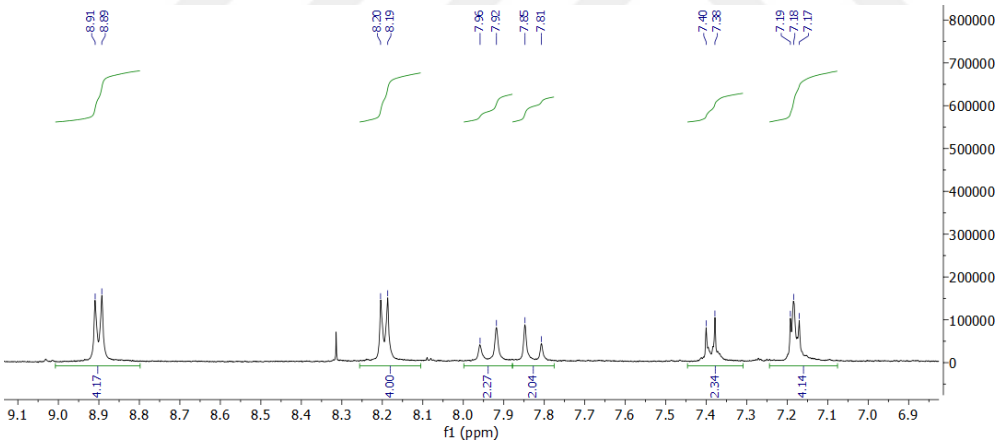

ANNEX-4 ^{1}H NMR Spectrum of Compound 5 (aromatic region, DMSO-*d*, 400 MHz)

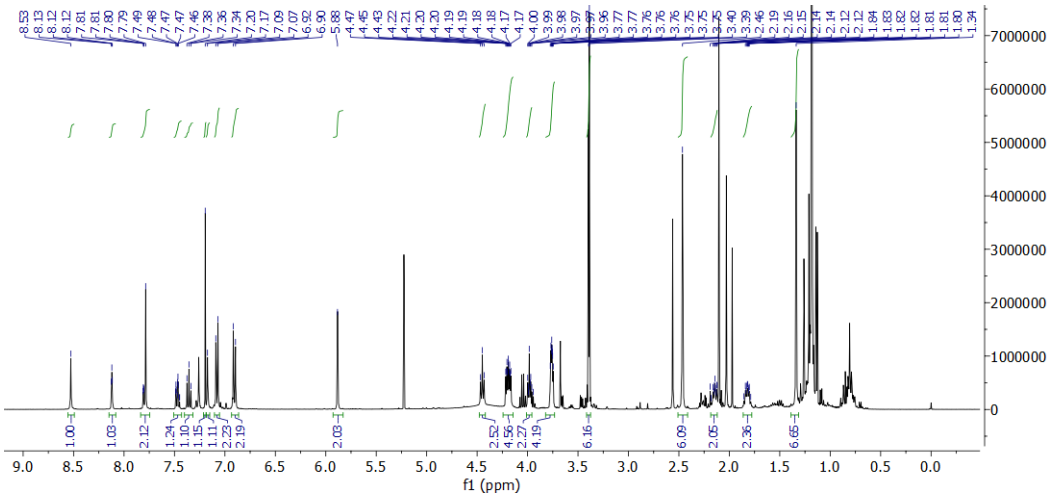

ANNEX-5 ^{1}H NMR Spcetrum of Compound 6 ($CDCl_3$, 400 MHz)

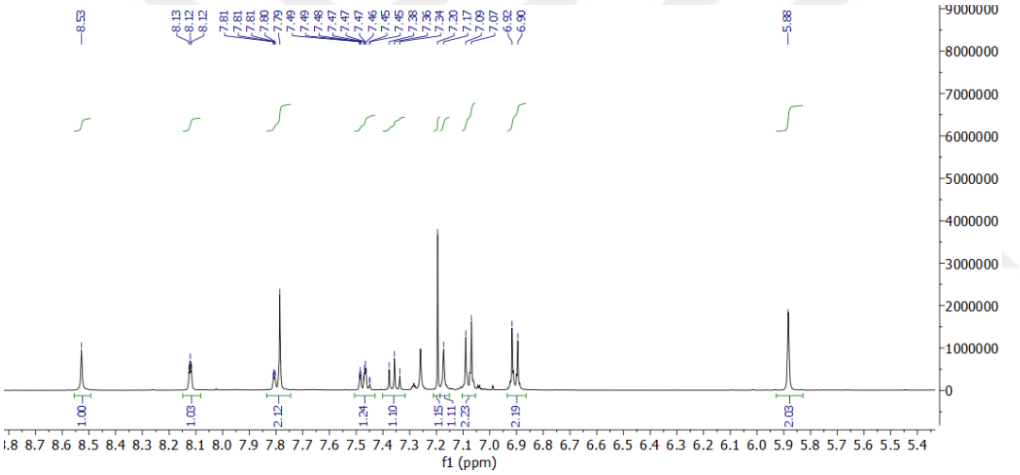

ANNEX-6 ^{1}H NMR Spcetrum of Compound 6 (aromatic region, $CDCl_3$, 400 MHz)